NeuroImage 202 (2019) 116078

Contents lists available at ScienceDirect

NeuroImage

journal homepage: www.elsevier.com/locate/neuroimage

Integration of spatio-temporal dynamics in emotion-cognition interactions: A simultaneous fMRI-ERP investigation using the emotional oddball task

Matthew Moore[a,*,1], Andrea T. Shafer[b,1], Reyhaneh Bakhtiari[c], Florin Dolcos[a,d,e,2,**], Anthony Singhal[c,f,***,2]

[a] *Beckman Institute for Advanced Science & Technology, University of Illinois at Urbana-Champaign, USA*
[b] *National Institute on Aging, USA*
[c] *Department of Psychology, University of Alberta, Canada*
[d] *Neuroscience Program, University of Illinois at Urbana-Champaign, USA*
[e] *Department of Psychology, University of Illinois at Urbana-Champaign, USA*
[f] *Neuroscience and Mental Health Institute, University of Alberta, Canada*

ARTICLE INFO

Keywords:
Affect
Individual differences
Neuroimaging
Personality

ABSTRACT

Although a large corpus of evidence has identified brain regions and networks involved in emotion-cognition interactions, it remains unclear how spatial and temporal dynamics of the mechanisms by which emotion interfaces with cognition are integrated. Capitalizing on multi-modal brain imaging approaches, we used simultaneous functional magnetic resonance imaging (fMRI) and event-related potential (ERP) recordings, to investigate the link between spatial and temporal aspects of processing in an emotional oddball task, and in relation to personality measures reflecting basic affective responses and emotion control. First, fMRI captured expected dorso-ventral dissociations, with greater response to targets in regions of dorsal brain networks (e.g., dorsolateral prefrontal cortex) and to emotional distracters in regions of ventral networks (e.g., ventrolateral prefrontal cortex, vlPFC). Also, ERP responses to targets were associated with a prominent P300, and responses to distracters with the late positive potential (LPP). Second, providing evidence for spatio-temporal integration of brain signals, ERP-informed fMRI analyses showed a link between LPP amplitude at parietal electrodes and the fMRI signal in the vlPFC, to emotional distraction. Third, regarding the link to personality measures, increased emotional arousability and attentional impulsiveness was associated with greater LPP differences between negative distracters and targets and enhanced response to negative distracters in the amygdala, respectively. Furthermore, we identified opposing relations between responses to emotional distraction and individual scores for cognitive reappraisal and self-control impulsiveness in posterior vlPFC. This suggests a greater engagement of this region in participants with reduced tendencies to employ reappraisal as a coping strategy and those with reduced ability to control impulsive responses during emotional distraction. Together, supporting the feasibility of integrating multi-dimensional approaches to clarify neural mechanisms of emotion-cognition interactions, these results point to convergence and complementarity between measures that differentially capture spatio-temporal dynamics of brain activity, and their associations with measures of individual differences in affective responses and control.

---

[*] Corresponding author. Beckman Institute for Advanced Science & Technology, University of Illinois at Urbana-Champaign, 405 North Mathews Avenue, Urbana, IL, 61801, USA.

[**] Corresponding author. Beckman Institute for Advanced Science & Technology, University of Illinois at Urbana-Champaign, 405 North Mathews Avenue, Urbana, IL, 61801, USA.

[***] Corresponding author. PhD Department of Psychology and Neuroscience and Mental Health Institute, University of Alberta, 11455, Saskatchewan Drive, Edmonton, AB, Canada.

E-mail addresses: mmoore16@illinois.edu (M. Moore), fdolcos@illinois.edu (F. Dolcos), asinghal@ualberta.ca (A. Singhal).

[1] Shared first-authorship.

[2] These authors contributed equally to the project.

https://doi.org/10.1016/j.neuroimage.2019.116078
Received 14 April 2019; Received in revised form 9 July 2019; Accepted 6 August 2019
Available online 7 August 2019

1. Introduction

Despite a growing body of evidence highlighting that emotion-cognition interactions elicit specific patterns of response in brain regions associated with major brain systems and networks (Barrett and Satpute, 2013; Dolcos et al., 2011; Iordan et al., 2013; Lindquist and Barrett, 2012; Seeley et al., 2007; Sylvester et al., 2012), it is unclear how the mechanisms by which emotion interfaces with cognition at various levels (from basic emotional responses to emotion control) are linked to *spatial* and *temporal* dynamics in the associated neural correlates. For example, it is not well understood how emotion processing, attentional control, and the interactions between these processes map onto the dynamic functioning of the associated brain mechanisms. Thus, there is a need to adopt comprehensive approaches through the utilization of multiple brain imaging modalities in order to elucidate the spatio-temporal dynamics of the neural mechanisms associated with emotion-cognition interactions in healthy functioning. In turn, this will provide insight into alterations associated with clinical disorders where emotion-cognition interactions are dysfunctional (e.g., anxiety, depression, post-traumatic stress disorders [PTSD], attention-deficit hyperactivity disorder [ADHD]). Clarification of these issues is central to generating novel neurobiological models and theories of emotion, and to advancing how cognitive and emotional dysfunctions are conceptualized, measured, treated, and prevented. Here, we used simultaneously acquired functional magnetic resonance imaging (fMRI) and electroencephalography/event-related potentials (EEG/ERPs) with a task of emotion-cognition interactions and personality measures indexing affective responses and emotion control in a sample of healthy young adults.

Presumably due to their relevance for survival, emotional stimuli tend to capture attentional resources more readily than neutral stimuli, which may result in distraction from task- or goal-relevant behavior. This can be detrimental to adaptive behavior, particularly in situations where one's survival is not in immediate danger, and hence the ability to limit the impact of emotional distraction is crucial to successful goal-relevant behavior. Consistent with this idea, on the one hand, difficulties in affective and attentional aspects of processing are often hallmarks of clinical disorders where goal-relevant behavior, such as decision making, might suffer (Banich et al., 2009; Dolcos et al., 2014). On the other hand, individual differences in factors supporting resilience and associated with enhanced cognitive control have been shown to predict lower symptoms of emotional distress (Dolcos et al., 2016; Moore et al., 2016, 2018), suggesting more adaptive responses to emotional challenges. Hence, characterizing the neural correlates of individual differences predicting susceptibility or resilience to emotional challenges is of key interest for promoting optimal emotion-cognition interactions and improving well-being.

Building upon clinical models of emotion-cognition interactions (Drevets and Raichle, 1998; Mayberg, 1997, 2006; Price and Drevets, 2012), fMRI studies with healthy participants, in which emotional information was presented as transient distraction during cognitive tasks (Anticevic et al., 2010; Chuah et al., 2010; Denkova et al., 2010; Diaz et al., 2011; Dolcos et al., 2011; Dolcos and McCarthy, 2006; Iordan et al., 2013; Oei et al., 2012), have shown that processing of task-irrelevant emotional distraction was linked to opposing patterns of activity in two large neural systems[3]: a dorsal executive neural system (DES) (showing *decreased* response) and a ventral affective system (VAS) (showing *increased* response). The dorsal system includes brain regions typically involved in executive cognitive functions, which are critical for executive-based attentional processing and the ability to maintain focus on goal-relevant information - e.g., dorsolateral prefrontal cortex (dlPFC) and lateral parietal cortex (LPC). The ventral system includes brain regions involved in emotion processing - e.g., ventrolateral prefrontal cortex (vlPFC), fusiform gyrus (FFG), amygdala (AMY), and ventral medial frontal cortex (vmPFC).

Understanding how the interfering effects of emotional distraction on ongoing cognitive processing are linked to transient interactions between these neural systems, in healthy participants (reviewed in Dolcos et al., 2011; Iordan et al., 2013), can inform future work with patient populations or populations at risk for mental disorders, to identify and treat possible break-downs in the mechanisms associated with these processes. However, fMRI is primarily advantageous for examining *where* changes occur in the brain, due to its high spatial resolution on the order of millimeters, but is less advantageous for examining *when* changes occur, due to the timing of hemodynamic response, which is on the order of seconds. Hence, elucidation of the link between spatial (*where*) and temporal (*when*) aspects of the neural correlates of emotion-cognition interactions requires integration of brain imaging methods with high spatial resolution, such as fMRI, with methods that allow for higher temporal resolution.

A common psychophysiological method for examining the temporal (*when*) aspects of brain function is EEG/ERP. Extant EEG studies highlight temporal markers associated with attentional control such as the P300 located over central and parietal electrodes[4] (Bledowski et al., 2004a; Campanella et al., 2013; Fabiani et al., 1987; Polich, 2007; Singhal et al., 2012), and temporal markers associated with emotion processing such as the late positive potential (LPP) located over occipital, temporal, and parietal electrodes (Dolcos and Cabeza, 2002; Schupp et al., 2004; Schupp et al., 2003; Singhal et al., 2012; Weinberg and Hajcak, 2010). For example, previous research has consistently shown that the P300 is associated with response to stimuli in cognitive-attentional paradigms such as the oddball task (Bledowski et al., 2004b; Bledowski et al., 2004a; Campanella et al., 2013), and that larger LPP amplitude is associated with processing of emotional compared to neutral images (Schupp et al., 2000, 2004). Importantly, these studies highlight differential temporal markers of attentional and emotional processing, which can be captured with a time scale on the order of milliseconds.

Whereas fMRI and EEG research have each separately identified spatial and temporal markers of brain function, it remains unclear how the dynamic process of emotion-cognition interactions maps onto the spatio-temporal changes of the associated neural mechanisms. For example, an open question in the literature is the role of regions such as the vlPFC in the impact of vs. coping with emotional distraction (Iordan et al., 2013). Consistent with the idea that the vlPFC is involved with multiple processes related to emotion, converging evidence from task-related and resting-state functional connectivity investigations

---

[3] It is important to note that while we do not treat DES and VAS as equivalent to brain networks, there are considerable overlaps between these larger neural systems and the large-scale functional networks (Iordan and Dolcos, 2017; Iordan et al., 2018). More specifically, the task-induced dorso-ventral dissociation between DES and VAS overlaps with the resting-state dissociations between the fronto-parietal control/central-executive/dorsal-attentional networks and the salience/cingulo-opercular/ventral-attentional networks, respectively (Bressler and Menon, 2010; Dosenbach et al., 2008; Dosenbach et al., 2007; Power et al., 2011; Seeley et al., 2007; Yeo et al., 2011).

[4] It should be noted that the more general term "P300" can refer to more specific variants of the P300, the P3a and P3b. The P3a component tends to have maximum amplitude over frontal and central locations on the scalp, and is associated with engagement of attention and processing of novelty (Polich, 2007). The P3b component tends to have maximum amplitude over central and parietal locations on the scalp, and is associated with response to improbable task-relevant events (Polich, 2007). In the present study, the focus was on the P3b due to the association this component has with task-relevant stimuli. Though P3a is commonly used for examining response to distracters in 3 condition oddball tasks (Polich, 2007; Polich and Criado, 2006), the present focus was on the emotional oddball variant, and thus the component of primary interest was the late positive potential (LPP) associated with emotional response (Schupp et al., 2000, 2004; Singhal et al., 2012).

points to the vlPFC as a site of rich functional heterogeneity, possibly linked to the overlap between different functional networks in this area (Cai et al., 2014; Gordon et al., 2014; Levy and Wagner, 2011; Power et al., 2011; Warren et al., 2014). However, the link between spatial and temporal aspects of processing associated with vlPFC responses to task-irrelevant emotional information (e.g., distraction vs. coping) is not clear. Specifically, it is not known how slow hemodynamic changes revealed by fMRI, are related to fast neuronal responses captured by fast methods, such as ERPs.

Consistent with the idea of complex associations between ERPs and fMRI responses, recent fMRI-EEG research has begun to use integrative analyses to examine the neural substrates of ERPs such as the LPP (Liu, Huang, McGinnis-Deweese, Keil and Ding, 2012) and P300 (Bledowski et al., 2004b). Such studies have identified correlations between the amplitude of LPP in response to unpleasant emotional pictures and blood oxygen level dependent (BOLD) response in the vlPFC, insula, and posterior cingulate cortex (Liu et al., 2012), and have modeled source localizations of P300 sub-components to parietal, inferior temporal, frontal, and insular areas (Bledowski et al., 2004b). These studies bring us closer to understanding how spatial and temporal aspects of brain functioning relate, but they have not directly targeted the interactions between emotion and attention, and thus it remains unclear how the spatio-temporal dynamics of these processes unfold.

Clarification of the links between spatial and temporal aspects of the brain mechanisms associated with emotion-cognition interactions depend not only on appropriate brain imaging techniques, but also on paradigms that reliably modulate neural activity in the brain systems of interest. Such a paradigm is the emotional oddball task, which has been used with both fMRI (Fichtenholtz et al., 2004; Wang et al., 2008a; Wang et al., 2008b; Wang et al., 2005; Yamasaki et al., 2002) and EEG/ERP (Briggs and Martin, 2009; Schluter and Bermeitinger, 2017; Singhal et al., 2012) recordings. This task involves identification of infrequent target stimuli (e.g., pictures of circles) in a stream of common stimuli (e.g., scrambled pictures), and other "distracter" stimuli, which might include emotional and neutral pictures (Fichtenholtz et al., 2004; Singhal et al., 2012; Wang et al., 2008a; Wang et al., 2008b; Wang et al., 2005; Yamasaki et al., 2002). Consistent with the dorso-ventral dissociations described in the DES-VAS framework, fMRI research using the emotional oddball task has shown greater response to targets compared to distracters in dorsal regions, such as the dlPFC and LPC, and greater response to distracters compared to targets in ventral regions, such as the vlPFC, FFG, and AMY (Fichtenholtz et al., 2004; Wang et al., 2008a; Wang et al., 2008b; Wang et al., 2005; Yamasaki et al., 2002). Also, consistent with the extant EEG literature, the emotional oddball task has been shown to capture the P300 and LPP responses (Singhal et al., 2012). Thus, using simultaneous fMRI-EEG during the emotional oddball task should work well to capture the spatio-temporal dynamics of the neural correlates underlying emotion-cognition interactions, and allow comprehensive investigation of individual differences in emotional and attentional domains.

A comprehensive account of the dynamics of emotion-cognition interactions should also include clarification of the variability that is explained by individual differences in emotional and attentional processes. For example, susceptibility to the initial impact of emotional distraction might vary as a function of individual differences in sensitivity to emotionally arousing stimuli that tend to capture attention (Denkova et al., 2010; Dolcos et al., 2013; Dolcos and McCarthy, 2006). Such variability might be captured by assessing personality traits that index an individual's tendency to experience emotions that they are exposed to in other people or in stimuli (Doherty, 1997), and how intense their emotional responses tend to be (Braithwaite, 1987). In addition to sensitivity to emotion eliciting stimuli in particular, variability might also be captured at the level of individual differences in attentional and self-control processes (Patton et al., 1995; Spinella, 2007). For instance, individuals who tend to have difficulty concentrating, as well as carefully thinking and planning, might be more susceptible to emotional distraction (Dolcos et al., 2013; Whiteside and Lynam, 2001). Finally, habitual cognitive control of emotion might also modulate the dynamics of emotion-cognition interactions. Specifically, an individual's tendency to change the way they think about a situation in order to change their emotions might, over time, alter the extent to which emotion eliciting situations and stimuli impact them (Gross and John, 2003). Overall, we might expect that individual differences indicating greater susceptibility to emotional distraction would be associated with greater VAS and LPP responses to emotional distracters, whereas individual differences indicating greater resilience to emotional distraction would show the opposite (Denkova et al., 2010; Dolcos et al., 2013; Dolcos and McCarthy, 2006).

The present investigation targeted spatio-temporal dynamics of brain function using a simultaneous fMRI-EEG approach in conjunction with an emotional oddball paradigm and measures of individual differences indexing susceptibility and resilience to emotionally arousing stimuli. This approach can integrate fMRI and EEG/ERP data to address the spatial dissociations captured in fMRI and the temporal responses captured with ERPs and clarify how the spatial (*where*) aspects of the neural correlates of emotion-cognition interactions are related to temporal (*when*) aspects. Based on the extant fMRI literature (Iordan et al., 2013), it was expected that dorsal brain regions would show greater response to targets compared to emotional distracters, while ventral regions would show an opposite pattern. Additionally, ventral regions would show particular sensitivity to emotional compared to neutral distracters. Based on the extant EEG literature (Bledowski et al., 2004b; Dolcos and Cabeza, 2002; Polich, 2007; Schupp et al., 2004; Schupp et al., 2003; Singhal et al., 2012; Weinberg and Hajcak, 2010), it was expected that ERP responses to targets would be associated with a prominent P300, and responses to distracters would be associated with a LPP, specifically with greater amplitude for emotional compared to neutral distracters. Furthermore, integrative analysis of fMRI and EEG would show convergence between these signals, with P300 amplitude being associated with BOLD in dorsal brain regions such as LPC (Bledowski et al., 2004a, 2004b) and LPP amplitude being associated with BOLD in ventral brain regions such as vlPFC (Liu et al., 2012). Notably, previous literature has suggested that amplitude of these ERPs is a feature associated with BOLD in these regions (Bledowski et al., 2004b; Liu et al., 2012), and hence this aspect of the ERPs was of particular interest for the present investigation. Finally, it was also expected that greater susceptibility to emotional distraction, as indexed by individual difference measures, would be associated with enhanced fMRI and EEG sensitivity to emotional distracters (Dolcos et al., 2013; Hajcak et al., 2010). More specifically, individuals with greater sensitivity to distraction (i.e., attentional impulsiveness) might show enhanced responses to emotional distracters in VAS regions implicated in bottom-up processing (Dolcos et al., 2013), and individuals who tend to have more intense emotional responses (i.e., higher levels of trait emotional arousability) might show greater differences in ERP responses to emotionally arousing stimuli (Hajcak et al., 2010). Conversely, individuals with traits suggesting increased tendencies to cope, such as greater cognitive and self-control (i.e., greater reappraisal, lower self-control impulsiveness), might engage less the regions that play a role in emotional distraction, such as vlPFC and occipito-temporal cortex (OTC) regions (Dolcos et al., 2006; Dolcos and McCarthy, 2006).

2. Methods

2.1. Participants

In the present study, twenty-two healthy young adults (18–31 years old, 13 females) underwent simultaneous fMRI-EEG recording. The experimental protocol was approved for ethical treatment of human participants by the Research Ethics Board at the University of Alberta, and all participants provided informed written consent.

2.2. *The emotion-cognition interactions task*

Simultaneous fMRI-EEG data were recorded while participants performed an emotional oddball task (Fig. 1), during which participants detected “oddball” target stimuli (shapes) presented in a string of standard (scrambled) and distracter (emotional and neutral) stimuli (Fichtenholtz et al., 2004; Singhal et al., 2012; Wang et al., 2008a; Wang et al., 2008b; Wang et al., 2005; Yamasaki et al., 2002). There were 60–72 target trials, 45-8 emotional (40 negative, 5–8 positive) distracter trials, 40 neutral distracter trials, and 536–704 scrambled image trials, each of which are displayed for 1250 ms. The number of target trials allowed for targets that followed targets as well as targets that followed distracters, to make the task less predictable for the participants. The inter-stimulus interval consisted of a fixation cross presented for 750 ms. The infrequent distracter stimuli (negative, positive, and neutral pictures) were selected from the International Affective Picture System (IAPS) (Lang et al., 2008) based on normative ratings for valence and arousal and were supplemented with in-house pictures used in previous studies (Singhal et al., 2012; Wang et al., 2005). Positive distracters were included to provide a rating anchor for negative and neutral distracters, and to avoid the induction of longer-lasting negative mood. After the oddball task, participants also rated the valence and arousal of emotional and neutral pictures, using a 9-point self-assessment manikin (Bradley and Lang, 1994; Singhal et al., 2012): 1 = very negative, 5 = neutral, 9 = very positive (for valence) and 1 = very low to 9 = very high (for arousal). Participants’ ratings of the distracters showed that negative distracters ($M = 2.59$, $SD = .68$) were rated as more negative than neutral distracters ($M = 5.37$, $SD = .25$; $t[20] = -17.58$, $p < .001$). Additionally, negative distracters were rated as more arousing ($M = 5.28$, $SD = 1.57$) than neutral distracters ($M = 2.33$, $SD = 1.33$; $t[20] = 12.44$, $p < .001$). For one participant, emotional ratings were not recorded, and hence could not be included in analyses involving rating scores. In the behavioral analyses, trials were excluded if they were incorrect and if reaction time (RT) data were ≤175 ms.

2.3. *Simultaneous fMRI-EEG: Data acquisition, preprocessing, and analysis*

2.3.1. *fMRI*

Scanning was conducted using a 1.5 T Sonata scanner. Following acquisition of the sagittal localizer and the 3D MPRAGE anatomical images (repetition time [TR] = 1600 ms, echo time [TE] = 3.82 ms, flip angle = 15°, field of view = 256 × 256 mm^2, volume size = 112 slices, voxel size = 1 × 1 × 1 mm^3), functional MRI data consisting of a series of T2*-weighted images were acquired using an echoplanar sequence (TR = 2000 ms, TE = 40 ms, flip angle = 90°, field of view = 256 × 256 mm^2, volume size = 28 slices, voxel size = 4 × 4 × 4 mm^3, descending slice acquisition). Due to a technical error during acquisition, two participants had truncated imaging sequences during one block, resulting in a loss of fMRI data for onsets of 5 trials of interest (i.e., 2 targets, 1 negative distracter, and 2 neutral distracters) for each of these participants. All preprocessing and analyses of fMRI data were performed using SPM12 (Wellcome Department of Cognitive Neurology, London, UK) and in-house MATLAB tools. Specifically, fMRI data were first corrected for differences in acquisition time between slices for each image. Second, each functional image was spatially realigned to the first image of each run to correct for head movement. Third, the functional images were transformed into the standard anatomical space defined by the Montreal Neurological Institute (MNI) template implemented in SPM12. Fourth, the normalized functional images were assessed using the Artifact Detection Tools (ART) toolbox (https://www.nitrc.org/projects/artifact_detect/). Functional volumes with excessive movement (z-score > ±6 for global mean signal value; > ±2 mm linear movement in the orthogonal planes; > ±0.05 radians of angular movement) were identified and a matrix of nuisance regressors was generated to be included in first-level analyses. No more than 35 functional volumes were removed for any one participant. Finally, the normalized functional images were spatially smoothed using an 8 mm Gaussian kernel, full-width-at-half-maximum (FWHM), to increase the signal-to-noise ratio.

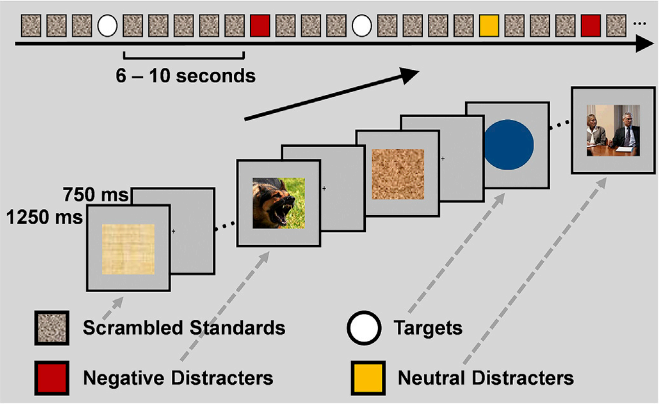

Fig. 1. Diagram of the Emotional Oddball Task. Participants detect “oddball” target stimuli presented in a string of standard (scrambled) and distracter (emotional and neutral) pictures.

At the first level, each participant’s preprocessed functional images were analyzed using an event-related design in the general linear model (GLM) framework, in which the onsets of target and distracter stimuli (i.e., negative, neutral, positive) were convolved with a canonical hemodynamic response function and included as the regressors of interest. Durations of the stimulus events were specified as the duration of stimulus presentation (i.e., 1250 ms). To control for motion-related artifacts, six motion parameters calculated during spatial realignment for each run were included in our GLM as regressors of no interest, along with the aforementioned nuisance regressors for functional images with excessive motion. These analyses generated contrast images identifying differential BOLD activation associated with each event of interest relative to baseline, as well as differences in activation between the events of interest. At the second level, the contrast images generated for each participant were entered into a within-participant ANOVA to test for general effects of conditions of interest (i.e., differential sensitivity to targets, negative distracters, and neutral distracters), to examine the differential BOLD activations at a group level using a whole-brain voxel-wise intensity threshold of $p < .005$ uncorrected for multiple comparisons and a cluster extent threshold corresponding to $p < .05$ corrected for multiple comparisons (family-wise error corrected, FWE). Furthermore, one-sample t-tests were used to target expected effects, such as the dorso-ventral dissociation for the most dissimilar conditions (i.e., targets vs. negative distracters).

Additionally, region of interest (ROI) statistical analyses (i.e., ANOVAs/t-tests and post-hoc analyses performed with Fisher’s Least Significant Difference tests) were performed using the individual activation maps and % signal change data extracted from ROIs and using the GLM framework for secondary voxel-wise analyses targeting sub-regional sensitivity to distracter type. The signal from the anatomical ROIs was constrained to significant functional clusters identified by the within-participant ANOVA for targets, negative distracters, and neutral distracters. This approach allowed for both anatomical specificity and a whole-brain statistical threshold. For the present analyses, ROIs for the DES included dlPFC and LPC, and for the VAS included vlPFC and FFG along with the surrounding OTC, and were broadly defined using masks from the Automated Anatomical Labeling (AAL) atlas (Tzourio-Mazoyer et al., 2002) to target each of these regions in each hemisphere (see Supplementary Materials for more details). For the primary ROI analyses, the fMRI signal was extracted from ROIs using a selective averaging approach, and averaged for each participant as a function of trial type (i.e., targets, negative distracters, neutral distracters) and time point (1 pre-stimulus and 7 post-stimulus onset time points). The number of time points before and after stimulus onset was selected in order to capture the entire hemodynamic response for each event onset. The signal was compared for each condition of interest for the time point covering the period of 6–8 s after stimulus onset. To ensure that effects were not driven by motion, trials in which a functional image had been identified as a motion outlier by ART were omitted from the analyses on extracted BOLD signals.

2.3.2. EEG

EEG data were acquired using a 64 channel Geodesic Sensor Net (Electrical Geodesics Inc., Eugene, OR), synchronized to the MRI clock, sampled at 250 Hz, and referenced to the vertex electrode (Cz). Electrooculogram (EOG) channels were located below the left and right eyes, and at the outer canthi of the left and right eyes. Data were processed using EEGLAB (Delorme and Makeig, 2004) and the fMRIB plug-in (Iannetti et al., 2005; Niazy et al., 2005). First, the fMRIB FASTR tool was used to remove MR gradient artifacts, which involved a low-pass filter of 70 Hz, up-sampling factor of 80, an averaging window of 30 artifact instances, and adaptive noise cancellation. The FASTR toolbox algorithm automatically calculated the number of residual artifact principal components to remove and conservatively removed components for each channel based on the amount of the total variance explained, how much of the variance is explained by each component, and the change in variance explained from one component to another (Niazy et al., 2005). Due to a technical error during acquisition, one block of EEG data from one participant did not have the fMRI TR markers that were used for the MR artifact removal step, and therefore this block was excluded from further analysis. Second, EEG data were low-pass finite impulse response (FIR) filtered at 30 Hz and high-pass FIR filtered at 0.1 Hz. Third, independent component analysis (ICA) was used to decompose the continuous EEG channel data, and components capturing the pulse and other artifacts were identified and removed based on visual inspection ($M = 5.77$ components; $SD = 1.45$). Fourth, the data were re-referenced to an average reference and the online reference (Cz) was added back to the data. Fifth, the data were up-sampled to 500 Hz and epochs for each condition were defined using a time window from 200 ms before stimulus onset to 824 ms after stimulus onset. This up-sampling combined with the selected epoch length was used in order to capture the expected ERP responses targeted in the present study (P300, LPP) with non-overlapping epochs that would have an appropriate number of samples for implementation of the wavelet denoising tool described below. Trials that still showed large microvolt amplitudes after data processing ($> \pm 150\ \mu V$), were excluded from analysis. ERP data from one participant was determined to have too few clean trials in the conditions of interest (<12 trials in target, negative distracter, and neutral distracter conditions), and therefore was excluded from analysis. Finally, targeted electrodes were filtered using a wavelet decomposition approach (Ahmadi and Quiroga, 2013), which is a common technique for enhancing extraction of task-related activity from average and single-trial ERP data. The wavelet decomposition approach was implemented using freely available automated software in MATLAB (Ahmadi and Quiroga, 2013), and was visually checked and manually adjusted in cases of poor decompositions (e.g., over-filtering). ERPs were targeted at central and parietal midline electrode locations within expected time-windows, consistent with those identified in previous studies using similar paradigms (Katayama and Polich, 1999; Singhal et al., 2012). Specifically, electrode Cz at a time window of 250–500 ms post-stimulus onset was used for P300, which is in line with the location and timing of when P300 responses have been identified in previous oddball studies (Katayama and Polich, 1999; Singhal et al., 2012; Warbrick et al., 2009), and electrode Pz at a time window of 550–800 ms post-stimulus onset was used for LPP, which is consistent with the location and timing of when LPP responses have been identified in previous studies using oddball and emotional picture tasks (Hajcak et al., 2010; Singhal et al., 2012). ERP analysis first involved a within-participant ANOVA, with factors of electrode (Cz, Pz), time window (250–500 ms, 550–800 ms), and condition (targets, negative distracters, neutral distracters). ANOVA results are reported with the Greenhouse-Geisser correction. Planned comparisons also included two-tailed paired t-tests on the average ERP amplitudes from each participant with a threshold of $p < .05$.

2.3.3. ERP-informed fMRI

Mean ERP amplitudes were extracted for each trial and used for parametric modulation analysis with fMRI BOLD signal. Within the P300 time window, mean amplitudes were extracted from electrode Cz. Within the LPP time window, mean amplitudes were extracted from Pz. Specifically, a P300 regressor was added to the design matrix for target onsets, and a LPP regressor was added for distracter onsets. Parametric modulation regressors containing trial-by-trial ERP amplitudes can be used to examine variability in the strength (i.e., amplitude) of the BOLD response across different instances of the same condition, beyond the effect of the task condition itself (Debener et al., 2006; Warbrick et al., 2009). Furthermore, the parametric modulation regressors were orthogonalized to address the collinearity of the typical event regressor and the parametric modulation regressor. The resulting GLM allowed for the examination of modulations in the BOLD response to targets associated with P300 amplitudes, and BOLD response to negative distracters associated with LPP amplitudes. Trials which did not have both fMRI and ERP data due to the aforementioned technical errors or due to data cleaning were not included in the GLM, and conditions which had too few trials per block (including positive distracters) were included in the model (both onset regressors and parametric modulation regressors) but were statistically removed (i.e., weighted as zero in the statistical contrasts). At the second level, the contrast images generated for each participant were entered into one-sample t-tests to examine the differential BOLD modulations at a group level using a whole-brain voxel-wise intensity threshold of $p < .005$ uncorrected for multiple comparisons and cluster extent threshold of 10 voxels (Bénar et al., 2007; Wirsich et al., 2014), unless otherwise stated.

2.4. Measures of individual differences

Personality measures included the Emotional Contagion Scale (ECS) (Doherty, 1997), Scale of Emotional Arousability (SEA) (Braithwaite, 1987), Barratt Impulsiveness Scale (BIS) (Patton et al., 1995; Spinella, 2007), and Emotion Regulation Questionnaire (ERQ) (Gross and John, 2003). Together, these scales allowed for measurement of individual differences in emotional (ECS, SEA, ERQ), and attentional domains (BIS). The ***Emotional Contagion Scale*** **(ECS)** (Doherty, 1997) is designed to assess people's susceptibility to "catching" *fear* (ECS_F), *anger* (ECS_A), *sadness* (ECS_S), *happiness* (ECS_H), and *love* (ECS_L), as well as emotions in general. It consists of 15 items rated on a 4-point scale ranging from 1 = "never" to 4 = "always." For the present study, the component of fear contagion (ECS_F) was of primary interest. The ***Scale of Emotional Arousability*** **(SEA)** allows for measurement of neuroticism, and comprises of items that focus specifically on emotional arousability (Braithwaite, 1987), or the intensity of emotional responses. The SEA contains 15 items concerning the way people typically behave, feel, or do things (e.g., "I get bored easily" and "I frequently get upset"). Items are rated on a 5-point scale from 1 = "no, this is very unlike me" to 5 = "yes, this is very like me." Components that can be assessed include *general emotionality* (SEA_E), *anger* (SEA_A), *timidity* (SEA_T), and *lack of control* (SEA_L). For the present study, the component of timidity (SEA_T) was of primary interest, because SEA_T assesses how easily frightened a person is, as well as whether a person has trouble making up their mind. The ***Emotion Regulation Questionnaire*** **(ERQ)** assesses the habitual engagement of two emotion regulation strategies, *reappraisal* (ERQ_R) and *suppression* (ERQ_S), using a 7-point scale that ranges from 1 = "strongly disagree" to 7 = "strongly agree." Examples of statements from the reappraisal dimension include "I control my emotions by changing the way I think about the situation I'm in," and statements from the suppression dimension include "I keep my emotions to myself" (Gross and John, 2003). For the present study, habitual reappraisal was of primary interest. Finally, the ***Barratt Impulsiveness Scale* (BIS)** measures the impulsive personality trait (Patton et al., 1995; Spinella, 2007). It consists of 30 items (e.g., "I plan tasks carefully," "I don't 'pay attention'") which may be scored to yield 6 first order factors (*attention*, BIS_Attn; *motor*, BIS_Mtr; *self-control*, BIS_SC; *cognitive complexity*, BIS_CC; *perseverance*, BIS_P; and *cognitive instability impulsiveness*, BIS_CI) and 3 second order factors (*attentional*, BIS_AI; *motor*, BIS_MI; and *nonplanning impulsiveness*, BIS_NPL). Each item is rated on a 4-point scale from 1 = "rarely/never" to 4 = "always." For the present study, the first order factors of attention (BIS_Attn) and self-control (BIS_SC) impulsiveness were of primary interest, because BIS_Attn is posited to measure impulsiveness related to "focusing on the task at hand" and BIS_SC is posited to measure impulsiveness related to "planning and thinking carefully" (Patton et al., 1995), which are both particularly relevant for performing cognitive tasks with emotional distraction.

Behavioral, fMRI, and ERP data were analyzed in conjunction with the individual difference measures introduced above, to examine associations among behavior, brain activity, and personality. For analyses of associations among behavioral variables and between behavior and ERPs, Pearson correlations were used and bootstrap 95% confidence intervals were calculated using 1000 bootstrap samples. For analyses of associations between behavioral variables and fMRI, group level one-sample *t*-tests were used within SPM12. Three participants were missing data: one was missing ratings and BIS data, one did not complete personality measures, and one had too few ERP trials, therefore analyses involving these measures did not include these participants. No individual differences analysis had a sample size lower than $n = 20$.

3. Results

3.1. Behavioral results

Participants tended to have high overall accuracy in responding to each category. Mean accuracy in response to targets was 80.43% ($SD = 16.79\%$), and over 90% in distracter and standard conditions (neutral distracters, $M = 91.48\%$, $SD = 12.95\%$; negative distracters, $M = 91.82\%$, $SD = 13.43\%$; positive distracters, $M = 91.59\%$, $SD = 14.91\%$; standards, $M = 91.30\%$, $SD = 13.50\%$). As expected, reaction times for negative distracters ($M = 438.11$ m, $SD = 119.84$ m) were greater than for neutral distracters ($M = 422.20$ m, $SD = 107.88$ m; $t[21] = 2.20$, $p = .039$). Due to the generally high rate of correct responses, and to maintain maximum statistical power, all trials (correct and incorrect) were used in the analyses of fMRI and EEG data.

3.2. fMRI results

Consistent with the expected DES and VAS engagement during the emotional oddball task, results from the whole-brain within-participant ANOVA showed differential sensitivity to targets, negative distracters, and neutral distracters in bilateral dlPFC, LPC, vlPFC, and OTC. More specifically, second level random-effects analyses of contrasts for the most dissimilar conditions (i.e., targets vs. negative distracters) clearly identified the expected pattern of greater response to targets compared to negative distracters in bilateral dlPFC and LPC, and the opposite pattern in bilateral vlPFC and OTC (Fig. 2; Table 1). Furthermore, repeated-measures ANOVAs computed on the percentage change in the MR signal from the targeted ROIs averaged across hemispheres showed that response was greater for targets in DES regions compared to negative and neutral distracters, and response to negative distracters was greater compared to targets and neutral distracters in VAS regions (Fig. 2). Specifically, a two-way 2 (neural system, dorsal vs. ventral) × 3 (targets vs. negative distracters vs. neutral distracters) ANOVA computed on the MR signal extracted from dorsal (dlPFC and anterior LPC [aLPC]) and ventral (vlPFC and OTC) regions yielded robust main effects of neural system ($F[1, 21] = 109.82$, $p < .001$, $\eta^2_p = .84$), and condition ($F[1.76, 36.90] = 8.73$, $p = .001$, $\eta^2_p = .29$), as well as a neural system × condition interaction ($F[1.75, 36.71] = 162.84$, $p < .001$, $\eta^2_p = .89$). One-way

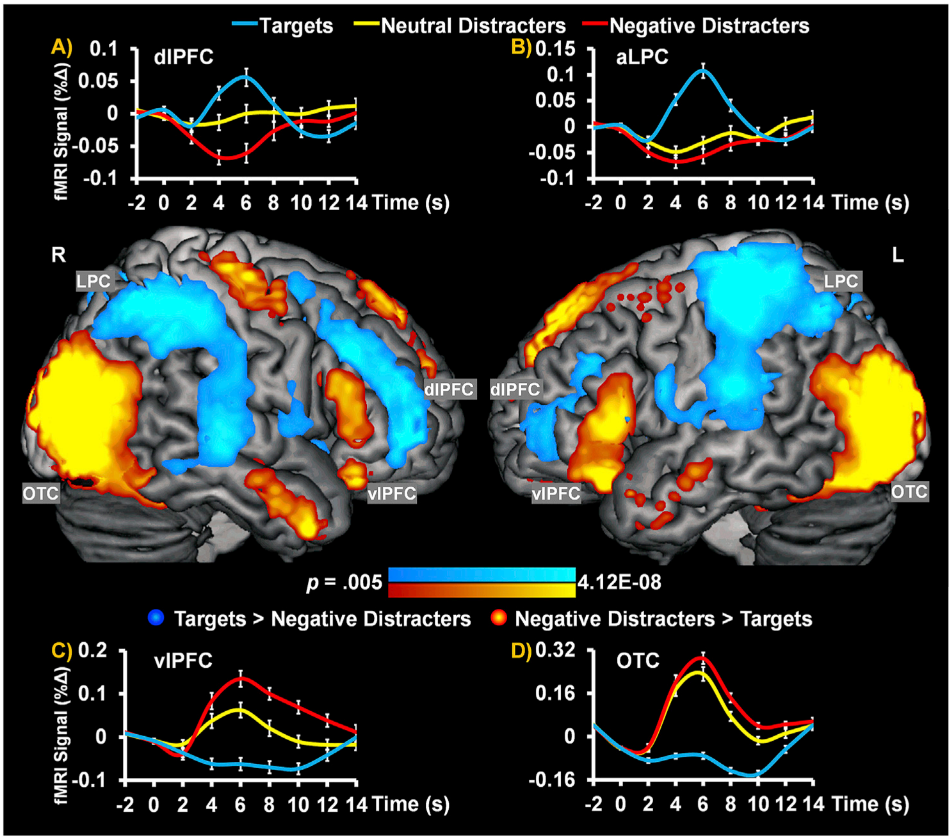

Fig. 2. Dorso-Ventral Dissociation between Responses to Targets and Negative Distracters. There were greater responses for targets compared to negative distracters in dlPFC (A) and aLPC (B), and the opposite pattern in vlPFC (C) and OTC (D). Activation maps are displayed with voxel-wise intensity threshold of $p < .005$ uncorrected, within a mask resulting from the whole-brain ANOVA contrast for regions sensitive to differences between targets, negative distracters, and neutral distracters, with height threshold $p < .005$ and extent threshold corresponding to $p < .05$ FWE corrected for multiple comparisons. Time course plots depict average BOLD % signal change from the contiguous clusters around peak locations within anatomical regions of interest. White bars on time course plots show the standard errors of the means. Left, L; right, R; dorsolateral prefrontal cortex, dlPFC; lateral parietal cortex, LPC; anterior lateral parietal cortex, aLPC; ventrolateral prefrontal cortex, vlPFC; occipito-temporal cortex, OTC.

Table 1

fMRI Results: Brain Regions Showing Sensitivity to Targets and Negative Distracters. This table identifies brain regions showing differential activity between the most dissimilar experimental conditions of targets and negative distracters, identified by *t*-tests significant above a voxel-wise intensity threshold of $p < .005$ uncorrected for multiple comparisons. These results were constrained by a mask from the whole-brain ANOVA contrast for regions sensitive to differences between targets, negative distracters, and neutral distracters, which had a height threshold $p < .005$ and extent threshold corresponding to $p < .05$ family-wise error corrected for multiple comparisons. To identify contiguous cluster sizes, identified statistical peaks were further masked by the intersection of Brodmann's area or label masks (dilated by a factor of 3 in 3D) and the left or right cerebrum or cerebellum mask (dilated by a factor of 1 in 3D) from the WFU Pickatlas (Lancaster et al., 2000; Maldjian et al., 2004; Maldjian et al., 2003). Statistical peaks outside of the masks or with masked clusters with extent <10 voxels were excluded. Left, L; right, R; Brodmann's area, BA.

Brain Region	Side	BA	MNI peak coordinates			*t*	Voxels	Volume (mm^3)
			x	y	z			
Targets > Negative Distracters								
Frontal Lobe								
Middle Frontal Gyrus	L	10	−28	48	4	6.99	186	11904
Middle Frontal Gyrus	L	9	−36	32	28	6.30	145	9280
Middle Frontal Gyrus	R	10	32	48	16	8.72	321	20544
Middle Frontal Gyrus	R	11	24	40	−12	6.41	87	5568
Middle Frontal Gyrus/	R	6	32	16	52	5.25	85	5440
Sub-Gyral	R	6	20	8	56	5.57		
Precentral Gyrus	L	6	−60	4	20	5.21	76	4864
Precentral Gyrus	R	9	40	28	32	9.40	301	19264
Precentral Gyrus	R	44	52	8	4	4.37	42	2688
Paracentral Lobule/	L	31	−8	−8	48	10.13	181	11584
Cingulate Gyrus	L	31	−12	−28	40	6.23		
Anterior Cingulate/	L	32	−20	32	8	7.17	262	16768
Cingulate Gyrus/	L	32	0	32	32	5.52		
Cingulate Gyrus	L	32	−20	16	28	5.41		
Anterior Cingulate/	L	24	−4	32	12	4.29	294	18816
Cingulate Gyrus	L	24	−16	−4	40	6.52		
Anterior Cingulate	R	33	12	16	20	5.05	37	2368
Cingulate Gyrus	R	32	16	16	36	4.73	380	24320
Cingulate Gyrus	R	24	20	8	44	6.90	299	19136
Parietal Lobe								
Postcentral Gyrus	L	3	−40	−24	56	14.69	465	29760
Postcentral Gyrus/	L	40	−52	−24	20	10.09	638	40832
Inferior Parietal Lobule	L	40	−36	−32	60	14.55		
Postcentral Gyrus	R	2	60	−20	32	4.90	227	14528
Postcentral Gyrus/	R	40	64	−24	20	5.48	528	33792
Inferior Parietal Lobule	R	40	48	−56	52	8.84		
Superior Parietal Lobule	L	7	−4	−60	64	7.65	339	21696
Precuneus	R	7	8	−68	52	9.89	188	12032
Precuneus	R	19	40	−72	44	5.32	26	1664
Cingulate Gyrus	L	23	0	−24	28	5.81	75	4800
Cingulate Gyrus	R	31	24	−44	28	4.93	23	1472
Posterior Cingulate	R	30	28	−64	8	6.15	11	704
Temporal Lobe								
Superior Temporal Gyrus	R	21	64	−24	−4	7.23	97	6208
Superior Temporal Gyrus	R	41	56	−24	4	6.45	111	7104
Middle Temporal Gyrus	R	20	56	−40	−12	3.79	10	640
Sub-Lobar								
Caudate (Caudate Body)	L		−12	20	16	3.92	66	4224
Caudate (Caudate Tail)	L		−40	−32	−8	5.02	12	768
Lentiform Nucleus (Putamen)	L		−24	8	16	6.90	166	10624
Lentiform Nucleus (Lateral Globus Pallidus)	R		16	8	−8	5.45	41	2624
Claustrum	L		−36	−20	4	4.71	177	11328
Claustrum	R		36	8	−8	6.72	119	7616
Insula	L	13	−40	−4	12	5.63	351	22464
Insula	R	13	56	−20	20	5.29	74	4736
Thalamus	L		0	−4	16	6.09	133	8512
Thalamus (Pulvinar)	L		−8	−28	16	7.66	66	4224
Thalamus (Lateral Dorsal Nucleus)	R		12	−16	16	5.71	31	1984
Extra-Nuclear	L		−32	−44	20	5.52	506	32384
Cerebellum								
Culmen	R		12	−52	−20	6.81	62	3968
Negative Distracters > Targets								
Frontal Lobe								
Superior Frontal Gyrus	L	8	−8	52	40	10.09	89	5696
Superior Frontal Gyrus	L	6	−12	24	64	4.76	41	2624
Superior Frontal Gyrus	R	9	12	60	28	5.57	33	2112
Superior Frontal Gyrus	R	8	4	52	40	4.71	37	2368
Medial Frontal Gyrus	L	10	−8	44	−16	7.24	43	2752
Middle Frontal Gyrus	L	6	−40	4	60	4.22	16	1024
Middle Frontal Gyrus	R	46	56	28	20	5.93	75	4800
Inferior Frontal Gyrus	L	47	−36	28	−16	9.30	140	8960
Inferior Frontal Gyrus	L	45	−52	24	4	9.04	94	6016

(*continued on next page*)

Table 1 (*continued*)

Brain Region	Side	BA	MNI peak coordinates			t	Voxels	Volume (mm^3)
			x	y	z			
Inferior Frontal Gyrus	R	47	36	28	−20	6.73	45	2880
Inferior Frontal Gyrus	R	9	40	12	24	3.95	24	1536
Precentral Gyrus	R	4	44	−12	64	7.29	67	4288
Parietal Lobe								
Postcentral Gyrus	R	1	36	−28	72	3.98	25	1600
Posterior Cingulate	L	31	−4	−52	24	6.36	47	3008
Posterior Cingulate	R	30	12	−52	16	4.86	192	12288
Temporal Lobe								
Superior Temporal Gyrus	L	38	−40	12	−36	4.22	45	2880
Superior Temporal Gyrus	R	38	44	12	−40	8.64	67	4288
Middle Temporal Gyrus/	L	21	−52	4	−28	4.23	29	1856
Inferior Temporal Gyrus	L	21	−60	−8	−16	4.11		
Middle Temporal Gyrus	L	39	−52	−72	20	7.81	210	13440
Middle Temporal Gyrus/	R	21	52	0	−28	5.19	105	6720
Sub-Gyral	R	21	52	−12	−20	5.72		
Middle Temporal Gyrus	R	39	48	−68	16	11.76	245	15680
Uncus	R	36	36	−4	−36	6.37	153	9792
Uncus	R	20	36	−12	−32	5.69	186	11904
Parahippocampal Gyrus (Hippocampus)	L		−24	−12	−24	6.60	64	4096
Parahippocampal Gyrus	L	27	−20	−32	−4	5.32	11	704
Parahippocampal Gyrus	R	35	24	−12	−28	7.88	80	5120
Occipital Lobe								
Lingual Gyrus/	L	18	−12	−52	4	4.75	631	40384
Middle Occipital Gyrus/	L	18	−36	−88	8	13.04		
Cuneus	L	18	−12	−100	16	12.05		
Lingual Gyrus/	L	17	−12	−92	4	10.14	192	12288
Inferior Occipital Gyrus	L	17	−20	−96	−4	9.91		
Lingual Gyrus/	R	19	16	−48	0	6.01	889	56896
Fusiform Gyrus/	R	19	36	−84	−8	12.33		
Middle Occipital Gyrus	R	19	32	−80	24	12.86		
Lingual Gyrus/	R	18	28	−76	−8	13.61	638	40832
Middle Occipital Gyrus	R	18	16	−96	16	13.27		
Fusiform Gyrus/	L	19	−24	−84	−12	13.79	766	49024
Middle Occipital Gyrus	L	19	−48	−80	8	13.38		
Cerebellum								
Culmen	L		−32	−36	−24	8.04	134	8576
Culmen	R		36	−40	−24	11.14	148	9472

ANOVAs computed on the percentage change in the MR signal for each condition of interest (targets vs. negative distracters vs. neutral distracters) yielded significant main effects in all four brain regions (dlPFC, $F[1.90, 39.91] = 13.98$, $p < .001$, $\eta^2_p = .40$; aLPC, $F[1.49, 31.22] = 36.03$, $p < .001$, $\eta^2_p = .63$; vlPFC, $F[1.75, 36.80] = 29.41$, $p < .001$, $\eta^2_p = .58$; OTC, $F[1.59, 33.41] = 120.74$, $p < .001$, $\eta^2_p = .85$). Results from post-hoc analyses were consistent with the idea that the negative distracters produced greater effects (i.e., deactivation, in the dorsal system vs. increased activation, in the ventral system) than targets in each region ($ps < .001$), and also greater effects than neutral distracters in most regions ($ps \leq .005$). In the aLPC, there was only a trend in the expected direction, $p = .065$, but see below and Supplementary Materials for analyses on signal from posterior LPC.

As expected, the secondary voxel-wise analysis targeting sub-regional sensitivity to distracter type within the broader parietal cortex confirmed that posterior LPC (e.g., BA 40) showed differential sensitivity to neutral vs. negative distracters (see Supplementary Fig. 1).

3.3. ERP results

Consistent with the expected P300 and LPP responses in the EEG data, deflections over central/parietal sites showed a peak response for targets in the earlier time window, and deflections over parietal sites showed a peak response for negative distracters in the later time window (Fig. 3). Specifically, an ANOVA for electrode × time window × condition showed main effects of electrode $F(1,20) = 10.06$, $p = .005$, $\eta^2_p = .34$, time window $F(1,20) = 4.80$, $p = .041$, $\eta^2_p = .19$, condition $F(1.46, 29.17) = 5.73$, $p = .014$, $\eta^2_p = .22$, and an electrode × condition interaction $F(1.71, 34.16) = 12.52$, $p < .001$, $\eta^2_p = .39$. Notably, the average P300 amplitude at Cz within the early time window was significantly greater in response to targets ($M = 2.98$, $SD = 3.44$) compared to negative distracters ($M = .25$, $SD = 2.39$; $t[20] = 4.64$, $p < .001$), and compared to neutral distracters ($M = -.26$, $SD = 2.38$; $t[20] = 4.62$, $p < .001$). Also, the average LPP amplitude at Pz within the late time window was significantly greater in response to negative distracters ($M = 2.54$, $SD = 2.74$) compared to targets ($M = .85$, $SD = 2.40$; $t[20] = 2.30$, $p = .033$), and neutral distracters ($M = .91$, $SD = 2.20$; $t[20] = 4.59$, $p < .001$) (Fig. 3).

3.4. ERP-informed fMRI results

Consistent with the expected ventral association, results from the ERP-informed fMRI analysis identified that modulation of the BOLD response in the vlPFC was associated with the LPP amplitude to negative distracters (Fig. 4 and Table 2). Interestingly, at the combined targeted threshold of $p < .005$ uncorrected and extent threshold of 10 voxels, the results did not identify significant modulations of the BOLD response associated with the P300 amplitude to targets. However, some peaks survived the intensity threshold of $p < .005$ at a lower extent threshold (see Supplementary Fig. 2 and Supplementary Table 1). For instance, such exploratory analyses identified that modulation of the BOLD response in the parietal cortex was associated with the P300 amplitude to targets, which is consistent with expected associations between P300 amplitude and BOLD signal (Bledowski et al., 2004a; Warbrick et al., 2009).

3.5. Behavioral, fMRI, and ERP associations with individual differences

Consistent with the idea that individuals with greater susceptibility to emotional distraction would respond more negatively to the negative

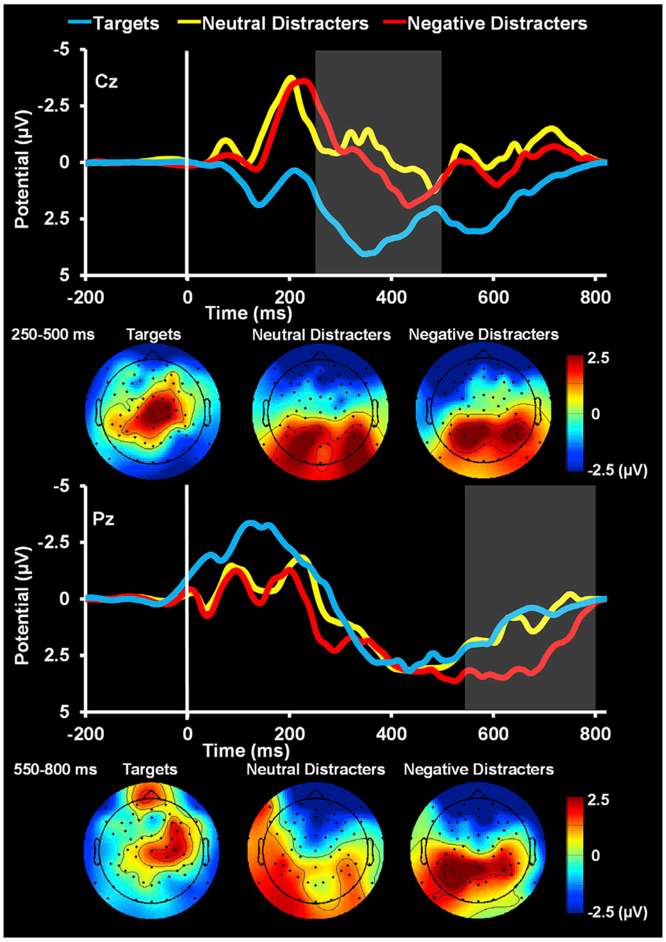

Fig. 3. ERP Response to Targets, Negative Distracters, and Neutral Distracters. ERP results showed the expected P300 response to targets peaking at central/parietal electrodes within the earlier time window, and greater LPP response for negative distracters compared to neutral distracters and targets over parietal electrodes within the later time window.

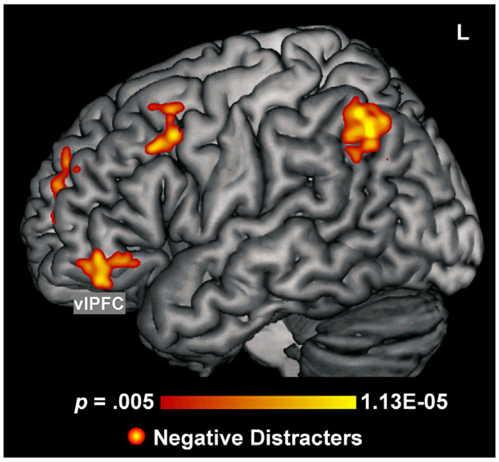

Fig. 4. BOLD Signal Modulations Associated with the LPP. ERP-informed fMRI results identified modulations of the BOLD response to negative distracters in several brain regions, including the vlPFC, linked to LPP amplitude. Displayed with a voxel-wise intensity threshold of $p < .005$ uncorrected, and an extent threshold of 10 voxels. Left, L; ventrolateral prefrontal cortex, vlPFC.

emotional distracters, and individuals with greater coping would respond less negatively, behavioral, fMRI, and ERP responses showed associations with individual differences in measures indexing aspects of emotional processing and attention. At the level of behavior, in line with the fact that the negative emotional distracters consisted of fear-inducing images (e.g., scenes of violence) (Lang et al., 2008; Singhal et al., 2012), greater sensitivity to fearful emotions, indicated by higher score on ECS_F, was associated with greater differences in valence ratings (Negative distracters reversed – Neutral distracters reversed), $r(18) = .67$, $p = .001$, bootstrap 95% confidence interval (CI) [0.36, 0.86] (Fig. 5A). At the level of neural correlates, both fMRI and ERP responses were associated with individual differences in aspects of emotion and attention indicating susceptibility to or resilience against emotional distraction. Supporting the idea that susceptibility to the initial impact of emotional distraction might vary as a function of how intense an individual's emotional responses tend to be, greater emotional arousability (SEA_T) was associated with greater differences between negative distracters and targets within the LPP time window (LPP Negative Distracters-Targets [µV]) $r(18) = .52$, $p = .018$, bootstrap 95% CI [0.27, 0.75] (Fig. 5B). Also in accord with the idea that individuals who tend to have difficulty concentrating might be more susceptible to emotional distraction (Dolcos et al., 2013; Whiteside and Lynam, 2001), greater attention impulsiveness (BIS_Attn) was associated with enhanced BOLD response to negative distracters in the AMY (Fig. 6A and Table 3).

Finally, supporting the idea that individuals that tend to engage more in coping show reduced response to emotional distraction, opposing relations between brain activity in response to emotional distraction and individual scores for cognitive reappraisal (ERQ_R) and self-control impulsiveness (BIS_SC) were identified in VAS-related regions, including the posterior vlPFC (BAs 44/45) and OTC (BAs 18/19). Specifically, greater levels of trait cognitive reappraisal (ERQ_R) were associated with decreased response to negative distracters, and greater levels of self-control impulsiveness (BIS_SC) were associated with increased response (Fig. 6B and Table 3). Notably, these findings are consistent with the idea that the posterior vlPFC plays a role in coping with emotional distraction (Dolcos et al., 2006; Iordan et al., 2013), and suggest that engagement of the OTC is also modulated by habitual levels of cognitive and self-control. Furthermore, trait reappraisal and self-control impulsiveness were inversely associated, $r(18) = -.53$, $p = .015$, bootstrap 95% CI [-0.81, -.16]. These results suggest that participants with reduced tendencies to engage reappraisal as a coping strategy and those with reduced ability to control impulsive responses had to engage more the posterior vlPFC and OTC while processing emotional distraction.

4. Discussion

The goal of the present study was to investigate spatio-temporal integration in the neural mechanisms associated with emotion-attention interactions. This was accomplished by capitalizing on simultaneously acquired fMRI and EEG data while participants performed an emotional oddball task, and by linking them to measures of individual differences in affective and attentional domains. First, the fMRI-EEG recordings showed the expected fMRI and ERP response patterns, and association between ERP amplitudes and modulation of the BOLD response, in expected regions. More specifically, fMRI captured the expected dorso-ventral dissociations for targets compared to negative distracters, and the expected ventral sensitivity to negative compared to neutral distracters. EEG captured the expected P300 response to targets, and the expected LPP response to distracters (particularly negative distracters). Second, associations between LPP and BOLD were identified in ventral regions such as vlPFC in response to negative distracters and, at an exploratory threshold, associations between P300 and BOLD were identified in dorsal regions such as LPC. Third, individual differences in personality were associated with behavioral and neural responses to emotional distraction. Differences in emotion and attention, suggesting greater susceptibility to emotional distraction, were associated with enhanced sensitivity to the negative emotional distracters. Behaviorally,

Table 2
ERP-informed fMRI Results for Negative Distracters. This table identifies brain regions showing modulation of BOLD response associated with ERP amplitude for the experimental condition of negative distracters. All peaks are reported using the criteria of a voxel-wise intensity threshold of $p < .005$ uncorrected for multiple comparisons. To identify contiguous cluster sizes, identified statistical peaks were further masked by the intersection of Brodmann's area or label masks (dilated by a factor of 3 in 3D) and the left or right cerebrum mask (dilated by a factor of 1 in 3D) from the WFU Pickatlas (Lancaster et al., 2000; Maldjian et al., 2003, 2004). Statistical peaks outside of the masks or with masked clusters with extent <10 voxels were excluded. Left, L; Brodmann's area, BA.

Brain Region	Side	BA	MNI peak coordinates			*t*	Voxels	Volume (mm^3)
			x	y	z			
LPP EEG-fMRI for Negative Distracters								
Frontal Lobe								
Superior Frontal Gyrus	L	9	−12	60	24	4.20	13	832
Superior Frontal Gyrus	L	10	−20	60	8	3.63	29	1856
Middle Frontal Gyrus	L	8	−48	16	40	3.92	23	1472
Inferior/Middle Frontal Gyrus	L	47/11	−44	40	−16	3.81	27	1728
Precentral Gyrus	L	9	−44	24	36	3.88	14	896
Parietal Lobe								
Angular Gyrus	L	39	−40	−60	44	5.49	38	2432

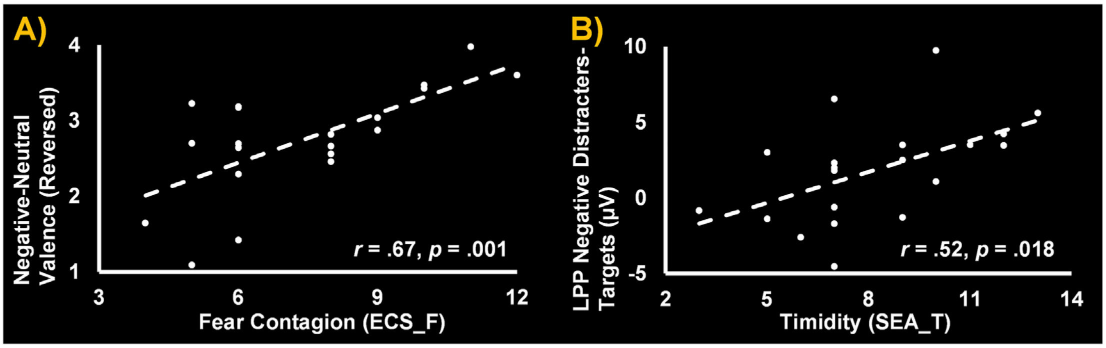

Fig. 5. Individual Differences Associated with Behavior and ERPs. (A) Greater levels of trait fear contagion (ECS_F) were associated with greater differences in valence ratings (Negative distracters reversed – Neutral distracters reversed). To increase interpretability for this comparison, valence scores were subtracted from 10 so that very negative ratings would be larger than neutral ratings before subtracting neutral distracter ratings from negative distracter ratings. (B) Greater timidity (SEA_T) was associated with greater differences between negative distracters and targets within the LPP time window (LPP Negative Distracters-Targets [µV]). Late positive potential, LPP.

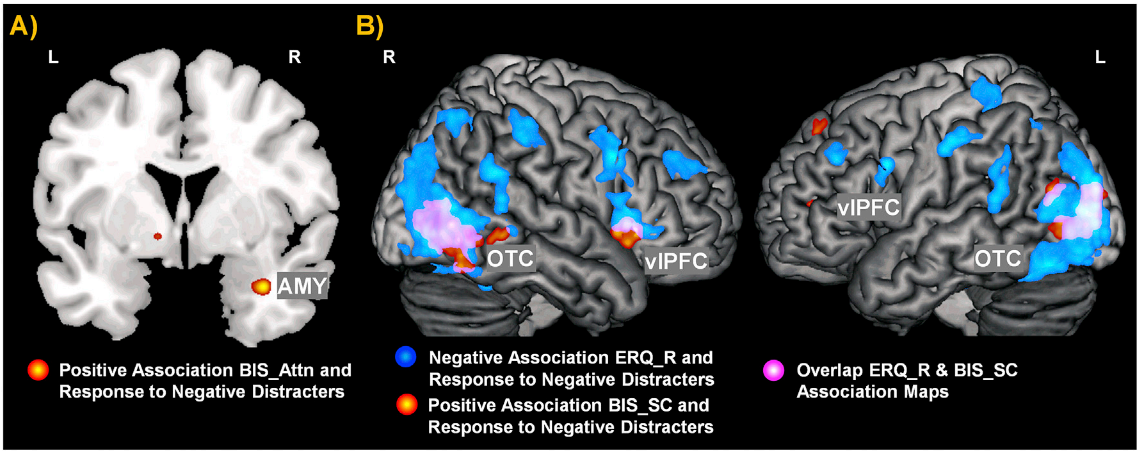

Fig. 6. Individual Differences Associated with fMRI. (A) Greater attention impulsivity (BIS_Attn) was associated with enhanced BOLD response to negative distracters in the AMY. (B) Greater levels of trait cognitive reappraisal (ERQ_R) were associated with decreased response to negative distracters in DES and vlPFC, as well as OTC, and greater levels of self-control impulsiveness (BIS_SC) were associated with increased response in vlPFC and OTC. Left, L; right, R; amygdala, AMY; dorsal executive system, DES; ventrolateral prefrontal cortex, vlPFC; occipito-temporal cortex, OTC.

greater sensitivity to fearful emotions was associated with greater differences in distracter image valence ratings. Psychophysiologically, both fMRI and ERP responses were associated with individual differences in emotion and attention. Greater emotional arousability was associated with greater ERP response to negative distracters (compared to targets) within the LPP time window. Higher attention impulsiveness was associated with greater BOLD response to negative distracters in the AMY, while greater levels of trait cognitive reappraisal were associated with reduced response to negative distracters in the vlPFC, which also positively associated with scores of self-control impulsiveness. The main findings are discussed in turn below.

Table 3

Personality Associations with fMRI Responses to Negative Distracters. This table identifies brain regions showing associations with attentional impulsiveness (BIS_Attn), self-control impulsiveness (BIS_SC), and cognitive reappraisal (ERQ_R). Regions shown meet the criteria of a voxel-wise intensity threshold of $p < .005$ uncorrected for multiple comparisons. To identify contiguous cluster sizes, identified statistical peaks were further masked by the intersection of Brodmann's area or label masks (dilated by a factor of 3 in 3D) and the left or right cerebrum or cerebellum mask (dilated by a factor of 1 in 3D) from the WFU Pickatlas (Lancaster et al., 2000; Maldjian et al., 2003, 2004). Statistical peaks outside of the masks or with masked clusters with extent <10 voxels were excluded. Left, L; right, R; Brodmann's area, BA.

Brain Region	Side	BA	MNI peak coordinates			*t*	Voxels	Volume (mm^3)
			x	*y*	*z*			
Individual Differences Associations with BOLD Response to Negative Distracters								
Positive Association BIS_Attn								
Temporal Lobe								
Superior Temporal Gyrus	L	22	−52	−16	−8	4.18	11	704
Parahippocampal Gyrus (Amygdala)	R		32	0	−24	4.15	12	768
Occipital Lobe								
Lingual Gyrus	R	19	24	−68	−4	4.33	10	640
Negative Association BIS_Attn								
Parietal Lobe								
Inferior Parietal Lobule	R	40	40	−48	44	4.61	34	2176
Cingulate Gyrus	R	31	20	−16	40	4.27	13	832
Temporal Lobe								
Parahippocampal Gyrus	L	28	−20	−20	−24	4.10	15	960
Positive Association BIS_SC								
Frontal Lobe								
Superior Frontal Gyrus/	L	8/9	−12	44	44	3.20	12	768
Medial Frontal Gyrus	L	8/9	−8	40	36	3.28		
Precentral Gyrus/Inferior Frontal Gyrus	R	44/47	52	20	0	4.62	44	2816
Anterior Cingulate	L	32	−20	36	12	3.99	10	640
Parietal Lobe								
Precuneus	R	7	12	−64	44	5.38	34	2176
Temporal Lobe								
Middle Temporal Gyrus	L	39	−48	−72	16	3.44	27	1728
Parahippocampal Gyrus	L	30	−16	−32	−8	5.15	19	1216
Occipital Lobe								
Middle Occipital Gyrus	L	19	−36	−64	12	4.65	28	1792
Middle Occipital Gyrus	L	18	−28	−88	8	4.15	82	5248
Middle Occipital Gyrus/	R	19	56	−64	−4	4.66	112	7168
Inferior Occipital Gyrus	R	19	44	−80	0	3.62		
Inferior Occipital Gyrus	L	19	−44	−76	0	3.97	89	5696
Cuneus	L	7	−12	−72	36	6.03	27	1728
Sub-Lobar								
Insula	R	13	40	16	−12	3.52	36	2304
Thalamus	L		−24	−16	12	3.86	11	704
Negative Association BIS_SC								
No suprathreshold voxels								
Positive Association ERQ_R								
No suprathreshold voxels								
Negative Association ERQ_R								
Frontal Lobe								
Medial Frontal Gyrus	L	6	0	8	52	4.43	83	5312
Medial Frontal Gyrus	R	9	28	40	20	4.44	37	2368
Middle Frontal Gyrus	L	8/9	−32	36	36	3.94	16	1024
Middle Frontal Gyrus	R	9	56	12	36	5.23	45	2880
Inferior Frontal Gyrus	L	9	−52	12	28	4.63	15	960
Inferior Frontal Gyrus	R	45	56	28	0	4.55	93	5952
Inferior Frontal Gyrus	R	44	60	16	12	3.70	65	4160
Precentral Gyrus	R	6	48	4	44	3.52	28	1792
Cingulate Gyrus	L	24	0	12	36	5.35	128	8192
Parietal Lobe								
Postcentral Gyrus	L	2	−48	−20	40	5.60	44	2816
Postcentral Gyrus	L	5	−32	−40	64	4.22	29	1856
Superior Parietal Lobule	L	7	−28	−52	44	4.61	22	1408
Superior Parietal Lobule/	R	7	32	−64	52	4.58	177	11328
Precuneus	R	7	20	−68	36	5.60		
Inferior Parietal Lobule	L	40	−32	−28	44	3.56	53	3392
Inferior Parietal Lobule	R	40	44	−28	40	5.55	59	3776
Supramarginal Gyrus	L	40	−64	−44	32	3.53	38	2432
Paracentral Lobule/	L	31	−4	−16	48	3.95	105	6720
Cingulate Gyrus	L	31	−12	−24	40	4.64		
Paracentral Lobule/	R	31	4	−28	48	4.06	57	3648
Cingulate Gyrus	R	31	8	−40	44	4.84		
Precuneus	L	7	−8	−48	48	5.35	62	3968
Precuneus	L	31	−16	−72	28	3.41	56	3584

(*continued on next page*)

Table 3 (*continued*)

Brain Region	Side	BA	MNI peak coordinates			*t*	Voxels	Volume (mm^3)
			x	*y*	*z*			
Cingulate Gyrus	L	23	−8	−24	28	3.25	16	1024
Cingulate Gyrus/	R	23	12	−20	24	4.24	36	2304
Posterior Cingulate	R	23	8	−32	24	5.36		
Temporal Lobe								
Superior Temporal Gyrus	L	22	−56	−44	16	5.27	33	2112
Superior Temporal Gyrus	R	41	48	−40	12	4.72	28	1792
Middle Temporal Gyrus	L	37	−48	−68	12	5.27	123	7872
Middle Temporal Gyrus	R	22	60	−36	0	3.47	51	3264
Middle Temporal Gyrus/	R	37	44	−60	4	5.71	176	11264
Inferior Temporal Gyrus	R	37	52	−68	0	5.11		
Parahippocampal Gyrus	L	27	−20	−32	−4	4.53	22	1408
Occipital Lobe								
Lingual Gyrus/	L	18	−16	−72	−4	4.52	267	17088
Middle Occipital Gyrus/	L	18	−32	−84	8	6.77		
Cuneus	L	18	−4	−80	32	3.74		
Middle Occipital Gyrus/	R	19	44	−68	12	5.24	283	18112
Inferior Occipital Gyrus	R	19	44	−80	−4	4.71		
Cuneus	L	17	−12	−84	16	3.40	24	1536
Cuneus	R	18	24	−84	32	4.10	115	7360
Sub-Lobar								
Caudate (Caudate Body)	L		−8	16	12	3.60	11	704
Lentiform Nucleus (Putamen)	L		−20	16	4	3.68	10	640
Lentiform Nucleus (Putamen)	R		24	0	12	3.86	35	2240
Insula	R	13	44	20	8	5.74	59	3776
Claustrum	R		32	8	12	3.69	33	2112
Thalamus (Anterior Nucleus)	R		8	−8	20	3.60	28	1792
Anterior/Posterior Lobe/Midbrain								
Culmen	R		40	−44	−24	5.71	109	6976
Declive	L		−40	−68	−20	5.84	71	4544
Declive	R		20	−76	−16	4.84	96	6144

4.1. Basic fMRI and ERP results

As expected, the fMRI results captured the opposing patterns of response in dorsal and ventral regions for targets compared to negative distracters, and the enhanced response particularly to negative compared to neutral distracters in ventral regions. These patterns are in line with previous investigations of the emotional oddball task (Fichtenholtz et al., 2004; Wang et al., 2008a; Wang et al., 2008b; Wang et al., 2005; Yamasaki et al., 2002), as well as other dual-tasks involving emotional distraction (Dolcos and McCarthy, 2006; Iordan and Dolcos, 2017; Iordan et al., 2013). Indeed, the dorso-ventral dissociations identified here are consistent with the idea that DES regions are engaged in goal-relevant processes such as attentional control and working memory, while the VAS regions are engaged in response to salient emotional stimuli such as emotionally arousing images (Dolcos et al., 2011; Dolcos and McCarthy, 2006; Iordan and Dolcos, 2017; Iordan et al., 2013). Furthermore, the opposing patterns observed in DES- and VAS-related regions converge with the behavioral reaction time results, suggesting that negative distracter images may have competed for and taken away attention-related resources from those engaged in performing the main task of detecting target stimuli. Notably, an advantage of these emotion-cognition interaction tasks is that they allow for investigation of dynamic interactions between large-scale brain systems, which might not be possible in paradigms that only target cognitive or emotional processes alone. As previously noted, in the current study, this was accomplished by examining the associations between the fMRI BOLD responses and the ERPs and individual difference measures, discussed below.

Turning to the ERP results, in response to the targets, a prominent P300 response was identified, and in response to distracters, LPP responses were identified. As expected, LPP waveforms showed larger amplitudes in response to the negative images compared to neutral images. This effect is in line with the longer reaction times in response to the negative images. The LPP has been shown to be sensitive to emotionally arousing pictures (Schupp et al., 2004), and this effect appears to be supported by the ratings data. Moreover, LPP response to negative emotional distracters may reflect the conscious awareness and salience of the images (Williams et al., 2007) that results from downstream processing of emotional information perhaps associated with engagement of VAS-related regions (e.g., amygdala) (Bradley et al., 2003). This idea is supported by the BOLD response patterns identified in VAS-related regions, which showed enhanced response particularly for negative emotional distracters.

4.2. ERP-informed fMRI results

The present findings show parallels and convergence between the separate fMRI and ERP analyses, and demonstrate how multi-modal recordings can be integrated for more comprehensive analyses. For example, the fMRI analysis captured greater response to negative distracters in vlPFC, and the ERP-informed fMRI showed associations between LPP amplitude and vlPFC BOLD. Additionally, fMRI analysis captured greater response to targets in dlPFC and LPC, and the ERP-informed fMRI analysis at an exploratory threshold pointed to associations between P300 amplitude and BOLD in dlPFC and LPC. The overall pattern of responses to negative distracters and VAS regions across temporal scales supports the idea that these regions are involved in processing salient and emotional distraction, and the pattern of target responses in DES regions across temporal scales is consistent with the idea that these regions subserve attentional and goal-relevant cognitive processing (Anticevic et al., 2010; Chuah et al., 2010; Denkova et al., 2010; Diaz et al., 2011; Dolcos et al., 2011; Dolcos and McCarthy, 2006; Iordan et al., 2013; Oei et al., 2012).

The results from fMRI BOLD and LPP responses to negative distracters confirm and expand on previous investigations of emotional distraction that have examined these neural correlates using fMRI and EEG separately (Dolcos and Cabeza, 2002; Fichtenholtz et al., 2004; Schupp et al., 2004; Wang et al., 2008a; Wang et al., 2008b; Weinberg and Hajcak, 2010; Yamasaki et al., 2002). Additionally, the association between vlPFC BOLD and LPP amplitude is consistent with results from previous multi-modal brain imaging studies of emotion processing (Liu et al., 2012). The associations identified with regions such as the posterior LPC (i.e., angular gyrus) also highlight possible dynamics that emerge during emotional distraction from an ongoing cognitive task. Specifically, the significant BOLD modulation in regions such as the vlPFC and posterior LPC associated with the LPP amplitude to negative distracters suggests that these structures are part of circuits or networks that contribute to the modulation of the cortical potential during emotional distraction. This possibility is further supported by the secondary analyses performed within the LPC, which identified posterior LPC sensitivity to distracter type. As noted previously, the vlPFC has been linked with both processing of emotional (Dolcos et al., 2011; Iordan et al., 2013) and salient information (Bressler and Menon, 2010; Corbetta et al., 2008; Seeley et al., 2007), as well as with affect regulation (Ochsner et al., 2004; Ochsner et al., 2012) and coping with emotional distraction (Dolcos et al., 2006; Iordan et al., 2013). Regions within the posterior LPC, such as the angular gyrus, play a key role in perception and attention, and have been posited to be a hub for integration of multisensory information (Seghier, 2013). Together, the association of these regions with the LPP is consistent with the idea that salient negative distracters tend to capture attention and that these hemodynamic and electrophysiological signals each capture indices of the associated response, across different spatial and temporal scales.

The association of the LPP with modulation of the BOLD response in the superior and middle frontal gyri is consistent with the idea that top-down processes can modulate the LPP (Hajcak et al., 2010). Since the emotional images in this task were distracters from the cognitive task of detecting targets, it is possible that the participants engaged in some form of top-down processing to respond to distracters and continue performing the task. This is a notable finding that points to the possible advantage of using an emotion-cognition interaction task to investigate the neural correlates of emotion and cognition, over tasks that target emotion or cognition alone. Additionally, the negative association between reappraisal and BOLD response to negative distracters in DES regions, such as the middle frontal gyrus, is consistent with the idea that these regions play a key role in top-down processes such as emotion control (Ochsner et al., 2012). Together, these results suggest that persons who tend to have enhanced responses to emotional distraction, indicated by greater LPP amplitudes and lower levels of habitual reappraisal, engaged more the DES during emotional distraction to maintain the high levels of performance in the task we observed in the overall sample. Future research could potentially investigate this effect more directly with explicit manipulations of top-down processes such as emotion regulation, and perhaps with more difficult tasks to increase variability in behavioral performance.

Although only apparent at an exploratory threshold, the association between modulation of BOLD and P300 amplitude in response to targets is in line with previous investigations of attention and executive functioning. For example, previous studies of the P300 have suggested that generators of this component are located in parietal and frontal locations, as well as regions such as the anterior cingulate cortex and medial temporal lobe (Linden, 2005). Consistent with these findings, the present exploratory results point to associations between BOLD modulation in these locations and the P300 amplitude. This suggests that regions within the DES and other areas might contribute to the P300, which is consistent with the large body of evidence highlighting the P300 as a signature of cognitive processes such as attention and working memory (Linden, 2005; Polich, 2007; Singhal and Fowler, 2004, 2005).

4.3. Behavioral, fMRI, and ERP associations with individual differences

Importantly, individual differences in emotional responses are suggested to be the rule rather than the exception (Hamann and Canli, 2004), and the use of multiple individual difference measures in the present study allowed for examining susceptibility to emotional distraction in both emotional and attentional domains. The association between sensitivity to fearful emotions and differences in valence ratings between negative and neutral distracters suggests that the negative images had a greater impact on individuals who were susceptible to fear responses. This result is consistent with the fact that the negative emotional distracters consisted of "fearful" images as opposed to other negative emotional categories (e.g., sad) (Lang et al., 2008; Singhal et al., 2012).

The association between greater attention impulsiveness and greater BOLD response to negative distracters in regions including the AMY and OTC is in line with the idea that VAS and related regions are sensitive to bottom-up information, such as emotionally salient stimuli that tend to capture attention (Dolcos et al., 2011). This result suggests that individuals that have more difficulty concentrating on the task at hand were more sensitive to emotionally distracting images. Additionally, greater levels of self-control impulsiveness were associated with enhanced response in VAS and related regions such as vlPFC/insula and OTC, which suggests that individuals with lower levels of self-control were impacted more by the negative emotional distracters. This result shows that individuals that have more difficulty thinking about tasks carefully were more sensitive to emotionally distracting pictures, and that this sensitivity mapped onto common and dissociable parts of the VAS where attention impulsiveness showed associations. Interestingly, the self-control impulsiveness association was primarily in the posterior area of the vlPFC and the insula, which is consistent with the idea that posterior vlPFC plays a role in coping with emotional distraction (Dolcos et al., 2006). This effect suggests that participants who typically engage less in self-control processes had to engage this area more during the presentation of negative emotional distracters to maintain performance on the task. This interpretation is further supported by the overlap that can be seen in Fig. 6B with the association between greater levels of trait cognitive reappraisal and lower response to negative distracters in the vlPFC.

Notably, the overlapping and opposing effects of self-control impulsiveness and cognitive reappraisal in posterior vlPFC suggest a spatial dissociation from effects that point to the initial impact of emotional distraction, such as the LPP association with anterior vlPFC. This dissociation between initial impact and subsequent coping is further supported by the positive association between scores of emotional arousability and the differences between negative distracters and targets within the LPP time window. As noted before, the vlPFC has been identified as an area of heterogeneity and a point of possible convergence between multiple identified networks (Cai et al., 2014; Gordon et al., 2014; Levy and Wagner, 2011; Power et al., 2011; Warren et al., 2014), and the dissociation of sub-regional roles is in line with the extant evidence targeting the vlPFC (Dolcos et al., 2006; Dolcos and McCarthy, 2006). Interestingly, a possible spatial dissociation is also suggested by the reappraisal association with lower response to negative distracters in anterior LPC, whereas the LPP is associated with posterior LPC areas including the angular gyrus. These results are in line with the extant evidence pointing to multiple networks converging in parietal areas (Cai et al., 2014; Gordon et al., 2014; Levy and Wagner, 2011; Power et al., 2011; Warren et al., 2014), and the role of parietal cortex in attention as well as cognitive control of emotion (Dolcos et al., 2011; Dolcos and McCarthy, 2006; Seghier, 2013). Overall, these results highlight sub-regional specificity that is uniquely identifiable through comprehensive multidimensional approaches that include multi-modal imaging in conjunction with assessment of individual differences. Future research building on this approach could help to further clarify the roles of regions where multiple networks seemingly overlap or interface, such as the vlPFC in the salience, ventral attention, and cingulo-opercular networks, and the parietal cortex in the fronto-parietal control, central-executive, dorsal-attentional networks (Bressler and Menon, 2010; Dosenbach et al., 2007, 2008; Power et al., 2011; Seeley et al., 2007; Yeo et al., 2011).

Together, the present findings are consistent with the idea that these psychophysiological signals can capture and dissociate different but related indices of brain activity, across spatial and temporal scales, and variability explained by individual differences. By examining the associations between the fMRI and ERP responses to an emotion-cognition interaction task, the present findings confirm and expand on previous studies that targeted cognitive and emotional processing separately (Bledowski et al., 2004b; Liu et al., 2012). Future work can build upon the present findings to further explore and manipulate emotion-cognition interactions, by examining factors such as changes in ERP latency, which is also a feature that associates with BOLD and might identify associations complementary to the ones found by examining ERP amplitude (Campanella et al., 2013; Warbrick et al., 2009). Manipulations of aspects such as cognitive load or emotion regulation could also be used in future work to further investigate dynamics in regions that are engaged in multiple roles, such as the vlPFC and parietal cortex.

Although the present study was in healthy young adults, the associations identified with measures of individual differences related to emotion and attention also point to possible implications for variability in these domains within the clinical spectrum. For example, the findings that greater emotional arousability was associated with greater ERP response to negative distracters (compared to targets) within the LPP time window, and that higher attention impulsiveness was associated with greater BOLD response to negative distracters in the AMY, are in line with previous evidence that enhanced response to the emotional distracters is apparent in adolescents with attention deficit-hyperactivity symptoms and affective disorders and patients with depression (Singhal et al., 2012; Wang et al., 2008a; Wang et al., 2008b). These results suggest that individual differences in sensitivity to emotional distraction can be examined across the spectrum from subclinical to clinical status, and that responses such as the LPP and AMY BOLD might be useful as targets for measuring and manipulating these responses to reduce emotional distraction.

4.4. Caveats

First, it is remarkable that these associations emerge despite multiple possible sources of variability and sensitivity that could be taken into account. For example, trial-by-trial measures from ERP can be sensitive to trial-by-trial variability, but this sensitivity can also lead to challenges with extracting signal from noise. Currently, there is not a clear consensus on which indices are optimal for integrative multi-modal brain imaging analyses, and hence these aspects should be considered carefully. Future research should confirm and expand on the EEG-fMRI associations identified here, using approaches such as the ones currently demonstrated as well as others that could possibly identify complementary associations (e.g., time-frequency analyses). Second, future work could also examine other ERP components, such as the P100, N200, P200, early posterior negativity (EPN), and the P3a to examine dissociable temporal markers of attentional and emotional processes. For example, it is notable that the negative and neutral distracter conditions appeared to elicit larger N200 components at Cz compared to the target condition, which might suggest modulated engagement of monitoring or attention during the presentation of distracting stimuli (Folstein and Van Petten, 2008). A broader time window for analyses of peak fMRI BOLD signal could also be used in future research to explore possible variability in responses or timing of dissociations across systems or regions (Dolcos and McCarthy, 2006; Iordan et al., 2018; Yamasaki et al., 2002). Additional comparisons investigating more subtle affects, such as targets following negative distracters, targets following neutral distracters, and targets following targets, are also important to explore in future investigations (Singhal et al., 2012).

5. Conclusion

In sum, the present report provides evidence demonstrating the integration of simultaneous bi-modal recording of fMRI and EEG, and highlights the parallel and converging results across the methodologies. The present results are consistent with the idea that dynamics captured early in electrophysiology and later in hemodynamic changes are associated with each other, and index related processing. The association between fMRI BOLD and ERP measures of response to distracters suggests that the VAS is engaged during salient distraction, particularly in response to negative emotional distraction. The fMRI and ERP responses to targets suggest that the DES is involved in attentional and executive functioning for goal-relevant processes. The present study highlights the spatio-temporal dynamics of emotion-cognition interactions, pointing to fMRI BOLD and ERP patterns that dissociated responses across conditions and were associated across modalities within condition. Furthermore, the individual differences results showed that individuals that have greater sensitivity to emotional distraction show enhanced VAS and LPP responses to negative emotional distracters, while those having greater control of emotion and attention show decreased responses in those measures. Finally, this investigation also provides evidence supporting sub-regional dissociations within the vlPFC, consistent with an anterior-posterior distribution of areas associated with the initial response vs. coping with emotional distraction, respectively. Collectively, the present results highlight the unique advantages of capitalizing on a multidimensional approach to investigate the spatio-temporal dynamics of emotion-cognition interactions and their link to individual differences in emotional and attentional domains.

Authors' note

F.D., A.T.S, and A.S. conceived the study; A.T.S. collected data; M.M. and F.D. planned the analytical approach, with feedback from A.T.S., A.S., and R.B.; M.M. performed the analyses; M.M. and F.D. wrote the manuscript, with feedback from A.T.S., A.S., and R.B, and all authors approved the content of the manuscript.

Declarations of interest

None.

Acknowledgements

The data was collected at the Peter S. Allen Centre at the University of Alberta supported by a Natural Sciences and Engineering Research Council Discovery Grant and a Canadian Foundation for Innovation Leaders Opportunity Fund infrastructure grant awarded to A.S. This work was conducted in part at the Beckman Institute for Advanced Science and Technology at the University of Illinois at Urbana-Champaign (UIUC-BI). During the preparation of this manuscript, M.M. was supported by Beckman Institute Predoctoral and Postdoctoral Fellowships, provided by the Beckman Foundation. F.D. was supported by a Helen Corley Petit Scholarship in Liberal Arts and Sciences and an Emanuel Donchin Professorial Scholarship in Psychology from the University of Illinois. The authors wish to thank Dr. Lihong Wang for feedback on the task design, and members of the Dolcos and Singhal Labs for assisting with data collection.

Appendix A. Supplementary data

Supplementary data to this article can be found online at https://doi.org/10.1016/j.neuroimage.2019.116078.

References

Ahmadi, M., Quiroga, R.Q., 2013. Automatic denoising of single-trial evoked potentials. NeuroImage 66, 672–680. https://doi.org/10.1016/j.neuroimage.2012.10.062.

Anticevic, A., Repovs, G., Barch, D.M., 2010. Resisting emotional interference: brain regions facilitating working memory performance during negative distraction. Cognit. Affect Behav. Neurosci. 10 (2), 159–173. https://doi.org/10.3758/CABN.10.2.159.

Banich, M.T., Mackiewicz, K.L., Depue, B.E., Whitmer, A.J., Miller, G.A., Heller, W., 2009. Cognitive control mechanisms, emotion and memory: a neural perspective with implications for psychopathology. Neurosci. Biobehav. Rev. 33 (5), 613–630. https://doi.org/10.1016/j.neubiorev.2008.09.010.

Barrett, L.F., Satpute, A., 2013. Large-scale brain networks in affective and social neuroscience: towards an integrative functional architecture of the brain. Curr. Opin. Neurobiol. 23 (3), 361–372. https://doi.org/10.1016/j.conb.2012.12.012.

Bénar, C.G., Schön, D., Grimault, S., Nazarian, B., Burle, B., Roth, M., Badier, J.M., Marquis, P., Liegeois-Chauvel, C., Anton, J.L., 2007. Single-trial analysis of oddball event-related potentials in simultaneous EEG-fMRI. Hum. Brain Mapp. 28 (7), 602–613. https://doi.org/10.1002/hbm.20289.

Bledowski, C., Prvulovic, D., Goebel, R., Zanella, F.E., Linden, D.E.J., 2004a. Attentional systems in target and distractor processing: a combined ERP and fMRI study. NeuroImage 22 (2), 530–540. https://doi.org/10.1016/j.neuroimage.2003.12.034.

Bledowski, C., Prvulovic, D., Hoechstetter, K., Scherg, M., Wibral, M., Goebel, R., Linden, D.E.J., 2004b. Localizing P300 generators in visual target and distractor processing: a combined event-related potential and functional magnetic resonance imaging study. J. Neurosci. 24 (42), 9353–9360. https://doi.org/10.1523/JNEUROSCI.1897-04.2004.

Bradley, M.M., Sabatinelli, D., Lang, P.J., Fitzsimmons, J.R., King, W., Desai, P., 2003. Activation of the visual cortex in motivated attention. Behav. Neurosci. 117 (2), 369–380. https://doi.org/10.1037/0735-7044.117.2.369.

Bradley, M.M., Lang, P.J., 1994. Measuring emotion: the self-assessment manikin and the semantic differential. J. Behav. Ther. Exp. Psychiatry 25 (1), 49–59. https://doi.org/10.1016/0005-7916(94)90063-9.

Braithwaite, V.A., 1987. The Scale of Emotional Arousability: bridging the gap between the neuroticism construct and its measurement. Psychol. Med. 17 (1), 217–225. https://doi.org/10.1017/S0033291700013106.

Bressler, S.L., Menon, V., 2010. Large-scale brain networks in cognition: emerging methods and principles. Trends Cogn. Sci. 14 (6), 277–290. https://doi.org/10.1016/j.tics.2010.04.004.

Briggs, K.E., Martin, F.H., 2009. Affective picture processing and motivational relevance: arousal and valence effects on ERPs in an oddball task. Int. J. Psychophysiol. 72 (3), 299–306. https://doi.org/10.1016/j.ijpsycho.2009.01.009.

Cai, W., Ryali, S., Chen, T., Li, C.S., Menon, V., 2014. Dissociable roles of right inferior frontal cortex and anterior insula in inhibitory control: evidence from intrinsic and task-related functional parcellation, connectivity, and response profile analyses across multiple datasets. J. Neurosci. 34 (44), 14652–14667. https://doi.org/10.1523/jneurosci.3048-14.2014.

Campanella, S., Bourguignon, M., Peigneux, P., Metens, T., Nouali, M., Goldman, S., Verbanck, P., De Tiege, X., 2013. BOLD response to deviant face detection informed by P300 event-related potential parameters: a simultaneous ERP-fMRI study. NeuroImage 71, 92–103. https://doi.org/10.1016/j.neuroimage.2012.12.077.

Chuah, L.Y.M., Dolcos, F., Chen, A.K., Zheng, H., Parimal, S., Chee, M.W.L., 2010. Sleep deprivation and interference by emotional distracters. Sleep 33 (10), 1305–1313. https://doi.org/10.1093/sleep/33.10.1305.

Corbetta, M., Patel, G., Shulman, G.L., 2008. The reorienting system of the human brain: from environment to theory of mind. Neuron 58 (3), 306–324. https://doi.org/10.1016/j.neuron.2008.04.017.

Debener, S., Ullsperger, M., Siegel, M., Engel, A.K., 2006. Single-trial EEG-fMRI reveals the dynamics of cognitive function. Trends Cogn. Sci. 10 (12), 558–563. https://doi.org/10.1016/j.tics.2006.09.010.

Delorme, A., Makeig, S., 2004. EEGLAB: an open source toolbox for analysis of single-trial EEG dynamics including independent component analysis. J. Neurosci. Methods 134 (1), 9–21. https://doi.org/10.1016/j.jneumeth.2003.10.009.

Denkova, E., Wong, G., Dolcos, S., Sung, K., Wang, L., Coupland, N., Dolcos, F., 2010. The impact of anxiety-inducing distraction on cognitive performance: a combined brain imaging and personality investigation. PLoS One 5 (11), e14150. https://doi.org/10.1371/journal.pone.0014150.

Diaz, M.T., He, G., Gadde, S., Bellion, C., Belger, A., Voyvodic, J.T., McCarthy, G., 2011. The influence of emotional distraction on verbal working memory: an fMRI investigation comparing individuals with schizophrenia and healthy adults. J. Psychiatr. Res. 45 (9), 1184–1193. https://doi.org/10.1016/j.jpsychires.2011.02.008.

Doherty, R.W., 1997. The emotional contagion scale: a measure of individual differences. J. Nonverbal Behav. 21 (2), 131–154. https://doi.org/10.1023/A:1024956003661.

Dolcos, F., Cabeza, R., 2002. Event-related potentials of emotional memory: encoding pleasant, unpleasant, and neutral pictures. Cognit. Affect Behav. Neurosci. 2 (3), 252–263. https://doi.org/10.3758/CABN.2.3.252.

Dolcos, F., Iordan, A.D., Dolcos, S., 2011. Neural correlates of emotion-cognition interactions: a review of evidence from brain imaging investigations. J. Cogn. Psychol. 23 (6), 669–694. https://doi.org/10.1080/20445911.2011.594433.

Dolcos, F., Iordan, A.D., Kragel, J., Stokes, J., Campbell, R., McCarthy, G., Cabeza, R., 2013. Neural correlates of opposing effects of emotional distraction on working memory and episodic memory: an event related fMRI investigation. Front. Psychol. 4 https://doi.org/10.3389/fpsyg.2013.00293.

Dolcos, F., Kragel, P., Wang, L., McCarthy, G., 2006. Role of the inferior frontal cortex in coping with distracting emotions. NeuroReport 17 (15), 1591–1594. https://doi.org/10.1097/01.wnr.0000236860.24081.be.

Dolcos, F., McCarthy, G., 2006. Brain systems mediating cognitive interference by emotional distraction. J. Neurosci. 26 (7), 2072–2079. https://doi.org/10.1523/JNEUROSCI.5042-05.2006.

Dolcos, F., Wang, L., Mather, M., 2014. Current research and emerging directions in emotion-cognition interactions. Front. Integr. Neurosci. 8, 83. https://doi.org/10.3389/fnint.2014.00083.

Dolcos, S., Hu, Y., Iordan, A.D., Moore, M., Dolcos, F., 2016. Optimism and the brain: trait optimism mediates the protective role of the orbitofrontal cortex gray matter volume against anxiety. Soc. Cogn. Affect. Neurosci. 11 (2), 263–271. https://doi.org/10.1093/scan/nsv106.

Dosenbach, N.U., Fair, D.A., Cohen, A.L., Schlaggar, B.L., Petersen, S.E., 2008. A dual-networks architecture of top-down control. Trends Cogn. Sci. 12 (3), 99–105. https://doi.org/10.1016/j.tics.2008.01.001.

Dosenbach, N.U., Fair, D.A., Miezin, F.M., Cohen, A.L., Wenger, K.K., Dosenbach, R.A., Fox, M.D., Snyder, A.Z., Vincent, J.L., Raichle, M.E., Schlaggar, B.L., Petersen, S.E., 2007. Distinct brain networks for adaptive and stable task control in humans. Proc. Natl. Acad. Sci. U. S. A. 104 (26), 11073–11078. https://doi.org/10.1073/pnas.0704320104.

Drevets, W.C., Raichle, M.E., 1998. Reciprocal suppression of regional cerebral blood flow during emotional versus higher cognitive processes: implications for interactions between emotion and cognition. Cognit. Emot. 12 (3), 353–385. https://doi.org/10.1080/026999398379646.

Fabiani, M., Gratton, G., Karis, D., Donchin, E., 1987. Definition, identification, and reliability of measurement of the P300 component of the event-related brain potential. Adv. Psychophysiol. 2, 1–78.

Fichtenholtz, H.M., Dean, H.L., Dillon, D.G., Yamasaki, H., McCarthy, G., LaBar, K.S., 2004. Emotion-attention network interactions during a visual oddball task. Cogn. Brain Res. 20 (1), 67–80. https://doi.org/10.1016/j.cogbrainres.2004.01.006.

Folstein, J.R., Van Petten, C., 2008. Influence of cognitive control and mismatch on the N2 component of the ERP: a review. Psychophysiology 45 (1), 152–170. https://doi.org/10.1111/j.1469-8986.2007.00602.x.

Gordon, E.M., Laumann, T.O., Adeyemo, B., Huckins, J.F., Kelley, W.M., Petersen, S.E., 2014. Generation and evaluation of a cortical area parcellation from resting-state correlations. Cerebr. Cortex 26 (1), 288–303. https://doi.org/10.1093/cercor/bhu239.

Gross, J.J., John, O.P., 2003. Individual differences in two emotion regulation processes: implications for affect, relationships, and well-being. J. Personal. Soc. Psychol. 85 (2), 348–362. https://doi.org/10.1037/0022-3514.85.2.348.

Hajcak, G., MacNamara, A., Olvet, D.M., 2010. Event-related potentials, emotion, and emotion regulation: an integrative review. Dev. Neuropsychol. 35 (2), 129–155. https://doi.org/10.1080/87565640903526504.

Hamann, S., Canli, T., 2004. Individual differences in emotion processing. Curr. Opin. Neurobiol. 14 (2), 233–238. https://doi.org/10.1016/j.conb.2004.03.010.

Iannetti, G.D., Niazy, R.K., Wise, R.G., Jezzard, P., Brooks, J.C.W., Zambreanu, L., Vennart, W., Matthews, P.M., Tracey, I., 2005. Simultaneous recording of laser-evoked brain potentials and continuous, high-field functional magnetic resonance imaging in humans. NeuroImage 28 (3), 708–719. https://doi.org/10.1016/j.neuroimage.2005.06.060.

Iordan, A.D., Dolcos, F., 2017. Brain activity and network interactions linked to valence-related differences in the impact of emotional distraction. Cerebr. Cortex 27 (1), 731–749. https://doi.org/10.1093/cercor/bhv242.

Iordan, A.D., Dolcos, S., Dolcos, F., 2013. Neural signatures of the response to emotional distraction: a review of evidence from brain imaging investigations. Front. Hum. Neurosci. 7 https://doi.org/10.3389/fnhum.2013.00200.

Iordan, A.D., Dolcos, S., Dolcos, F., 2018. Brain activity and network interactions in the impact of internal emotional distraction. Cerebr. Cortex. https://doi.org/10.1093/cercor/bhy129.

Katayama, J., Polich, J., 1999. Auditory and visual P300 topography from a 3 stimulus paradigm. Clin. Neurophysiol. 110 (3), 463–468. https://doi.org/10.1016/S1388-2457(98)00035-2.

Lancaster, J.L., Woldorff, M.G., Parsons, L.M., Liotti, M., Freitas, E.S., Rainey, L., Kochunov, P.V., Nickerson, D., Mikiten, S.A., Fox, P.T., 2000. Automated Talairach Atlas labels for functional brain mapping. Hum. Brain Mapp. 10 (3), 120–131. https://doi.org/10.1002/1097-0193(200007)10:3<120::Aid-Hbm30>3.0.Co;2-8.

Lang, P.J., Bradley, M.M., Cuthbert, B.N., 2008. International Affective Picture System (IAPS): Affective Ratings of Pictures and Instruction Manual. University of Florida, Gainesville, FL. Technical Report A-8.

Levy, B.J., Wagner, A.D., 2011. Cognitive control and right ventrolateral prefrontal cortex: reflexive reorienting, motor inhibition, and action updating. Ann. N. Y. Acad. Sci. 1224, 40–62. https://doi.org/10.1111/j.1749-6632.2011.05958.x.

Linden, D.E.J., 2005. The P300: where in the brain is it produced and what does it tell us? The Neuroscientist 11 (6), 563–576. https://doi.org/10.1177/1073858405280524.

Lindquist, K., Barrett, L.F., 2012. A functional architecture of the human brain: emerging insights from the science of emotion. Trends Cogn. Sci. 16 (11), 533–540. https://doi.org/10.1016/j.tics.2012.09.005.

Liu, Y., Huang, H., McGinnis-Deweese, M., Keil, A., Ding, M., 2012. Neural substrate of the late positive potential in emotional processing. J. Neurosci. 32 (42), 14563–14572. https://doi.org/10.1523/jneurosci.3109-12.2012.

Maldjian, J.A., Laurienti, P.J., Burdette, J.H., 2004. Precentral gyrus discrepancy in electronic versions of the Talairach Atlas. NeuroImage 21 (1), 450–455. https://doi.org/10.1016/j.neuroimage.2003.09.032.

Maldjian, J.A., Laurienti, P.J., Kraft, R.A., Burdette, J.H., 2003. An automated method for neuroanatomic and cytoarchitectonic atlas-based interrogation of fMRI data sets. NeuroImage 19 (3), 1233–1239. https://doi.org/10.1016/S1053-8119(03)00169-1.

Mayberg, H.S., 1997. Limbic-cortical dysregulation: a proposed model of depression. J. Neuropsychiatry Clin. Neurosci. 9 (3), 471–481. https://doi.org/10.1176/jnp.9.3.471.

Mayberg, H.S., 2006. Defining neurocircuits in depression. Psychiatr. Ann. 36 (4), 259–268. https://doi.org/10.1016/j.biopsych.2007.01.013.

Moore, M., Culpepper, S., Phan, K.L., Strauman, T.J., Dolcos, F., Dolcos, S., 2018. Neurobehavioral mechanisms of resilience against emotional distress: an integrative brain-personality-symptom approach using structural equation modeling. Personal. Neurosci. 1, 1–10. https://doi.org/10.1017/pen.2018.11.

Moore, M., Iordan, A.D., Hu, Y., Kragel, J.E., Dolcos, S., Dolcos, F., 2016. Localized or diffuse: the link between prefrontal cortex volume and cognitive reappraisal. Soc. Cogn. Affect. Neurosci. 11 (8), 1317–1325. https://doi.org/10.1093/scan/nsw043.

Niazy, R.K., Beckmann, C.F., Iannetti, G.D., Brady, J.M., Smith, S.M., 2005. Removal of fMRI environment artifacts from EEG data using optimal basis sets. NeuroImage 28 (3), 720–737. https://doi.org/10.1016/j.neuroimage.2005.06.067.

Ochsner, K.N., Ray, R.D., Cooper, J.C., Robertson, E.R., Chopra, S., Gabrieli, J.D., Gross, J.J., 2004. For better or for worse: neural systems supporting the cognitive down- and up-regulation of negative emotion. NeuroImage 23 (2), 483–499. https://doi.org/10.1016/j.neuroimage.2004.06.030.

Ochsner, K.N., Silvers, J.A., Buhle, J.T., 2012. Functional imaging studies of emotion regulation: a synthetic review and evolving model of the cognitive control of emotion. Ann. N. Y. Acad. Sci. 1251, E1–E24. https://doi.org/10.1111/j.1749-6632.2012.06751.x.

Oei, N.Y., Veer, I.M., Wolf, O.T., Spinhoven, P., Rombouts, S.A., Elzinga, B.M., 2012. Stress shifts brain activation towards ventral 'affective' areas during emotional distraction. Soc. Cogn. Affect. Neurosci. 7 (4), 403–412. https://doi.org/10.1093/scan/nsr024.

Patton, J.H., Stanford, M.S., Barratt, E.S., 1995. Factor structure of the Barratt Impulsiveness Scale. J. Clin. Psychol. 51 (6), 768–774. https://doi.org/10.1002/1097-4679(199511)51:6<768::Aid-Jclp2270510607>3.0.Co;2-1.

Polich, J., 2007. Updating P300: an integrative theory of P3a and P3b. Clin. Neurophysiol. 118 (10), 2128–2148. https://doi.org/10.1016/j.clinph.2007.04.019.

Polich, J., Criado, J.R., 2006. Neuropsychology and neuropharmacology of P3a and P3b. Int. J. Psychophysiol. 60 (2), 172–185. https://doi.org/10.1016/j.ijpsycho.2005.12.012.

Power, J.D., Cohen, A.L., Nelson, S.M., Wig, G.S., Barnes, K.A., Church, J.A., Vogel, A.C., Laumann, T.O., Miezin, F.M., Schlaggar, B.L., Petersen, S.E., 2011. Functional network organization of the human brain. Neuron 72 (4), 665–678. https://doi.org/10.1016/j.neuron.2011.09.006.

Price, J.L., Drevets, W.C., 2012. Neural circuits underlying the pathophysiology of mood disorders. Trends Cogn. Sci. 16 (1), 61–71. https://doi.org/10.1016/j.tics.2011.12.011.

Schluter, H., Bermeitinger, C., 2017. Emotional oddball: a review on variants, results, and mechanisms. Rev. Gen. Psychol. 21 (3), 179–222. https://doi.org/10.1037/gpr0000120.

Schupp, H.T., Cuthbert, B.N., Bradley, M.M., Cacioppo, J.T., Ito, T., Lang, P.J., 2000. Affective picture processing: the late positive potential is modulated by motivational relevance. Psychophysiology 37 (2), 257–261.

Schupp, H.T., Cuthbert, B.N., Bradley, M.M., Hillman, C.H., Hamm, A.O., Lang, P.J., 2004. Brain processes in emotional perception: motivated attention. Cognit. Emot. 18 (5), 593–611. https://doi.org/10.1080/02699930341000239.

Schupp, H.T., Junghofer, M., Weike, A.I., Hamm, A.O., 2003. Emotional facilitation of sensory processing in the visual cortex. Psychol. Sci. 14 (1), 7–13. https://doi.org/10.1111/1467-9280.01411.

Seeley, W.W., Menon, V., Schatzberg, A.F., Keller, J., Glover, G.H., Kenna, H., Reiss, A.L., Greicius, M.D., 2007. Dissociable intrinsic connectivity networks for salience processing and executive control. J. Neurosci. 27 (9), 2349–2356. https://doi.org/10.1523/jneurosci.5587-06.2007.

Seghier, M.L., 2013. The angular gyrus: multiple functions and multiple subdivisions. The Neuroscientist 19 (1), 43–61. https://doi.org/10.1177/1073858412440596.

Singhal, A., Fowler, B., 2004. The differential effects of Sternberg short- and long-term memory scanning on the late Nd and P300 in a dual-task paradigm. Cogn. Brain Res. 21 (1), 124–132. https://doi.org/10.1016/j.cogbrainres.2004.06.003.

Singhal, A., Fowler, B., 2005. The effects of memory scanning on the late Nd and P300: an interference study. Psychophysiology 42 (2), 142–150. https://doi.org/10.1111/j.1469-8986.2005.00275.x.

Singhal, A., Shafer, A.T., Russell, M., Gibson, B., Wang, L., Vohra, S., Dolcos, F., 2012. Electrophysiological correlates of fearful and sad distraction on target processing in adolescents with attention deficit-hyperactivity symptoms and affective disorders. Front. Integr. Neurosci. 6, 119. https://doi.org/10.3389/fnint.2012.00119.

Spinella, M., 2007. Normative data and a short form of the Barratt Impulsiveness Scale. Int. J. Neurosci. 117 (3), 359–368. https://doi.org/10.1080/00207450600588881.

Sylvester, C., Corbetta, M., Raichle, M., Rodebaugh, T., Schlaggar, B., Sheline, Y., Zorumski, C., Lenze, E., 2012. Functional network dysfunction in anxiety and anxiety disorders. Trends Neurosci. 35 (9), 527–535. https://doi.org/10.1016/j.tins.2012.04.012.

Tzourio-Mazoyer, N., Landeau, B., Papathanassiou, D., Crivello, F., Etard, O., Delcroix, N., Mazoyer, B., Joliot, M., 2002. Automated anatomical labeling of activations in SPM using a macroscopic anatomical parcellation of the MNI MRI single-subject brain. NeuroImage 15 (1), 273–289. https://doi.org/10.1006/nimg.2001.0978.

Wang, L., Krishnan, K.R., Steffens, D.C., Potter, G.G., Dolcos, F., McCarthy, G., 2008a. Depressive state- and disease-related alterations in neural responses to affective and executive challenges in geriatric depression. Am. J. Psychiatry 165 (7), 863–871. https://doi.org/10.1176/appi.ajp.2008.07101590.

Wang, L., Labar, K.S., Smoski, M., Rosenthal, M.Z., Dolcos, F., Lynch, T.R., Krishnan, R.R., McCarthy, G., 2008b. Prefrontal mechanisms for executive control over emotional distraction are altered in major depression. Psychiatry Res. Neuroimaging 163 (2), 143–155. https://doi.org/10.1016/j.pscychresns.2007.10.004.

Wang, L., McCarthy, G., Song, A.W., Labar, K.S., 2005. Amygdala activation to sad pictures during high-field (4 tesla) functional magnetic resonance imaging. Emotion 5 (1), 12–22. https://doi.org/10.1037/1528-3542.5.1.12.

Warbrick, T., Mobascher, A., Brinkmeyer, J., Musso, F., Richter, N., Stoecker, T., Fink, G.R., Shah, N.J., Winterer, G., 2009. Single-trial P3 amplitude and latency informed event-related fMRI models yield different BOLD response patterns to a target detection task. NeuroImage 47 (4), 1532–1544. https://doi.org/10.1016/j.neuroimage.2009.05.082.

Warren, D.E., Power, J.D., Bruss, J., Denburg, N.L., Waldron, E.J., Sun, H., Petersen, S.E., Tranel, D., 2014. Network measures predict neuropsychological outcome after brain injury. Proc. Natl. Acad. Sci. U. S. A. 111 (39), 14247–14252. https://doi.org/10.1073/pnas.1322173111.

Weinberg, A., Hajcak, G., 2010. Beyond good and evil: the time-course of neural activity elicited by specific picture content. Emotion 10 (6), 767–782. https://doi.org/10.1037/a0020242.

Whiteside, S.P., Lynam, D.R., 2001. The Five Factor Model and impulsivity: using a structural model of personality to understand impulsivity. Personal. Individ. Differ. 30 (4), 669–689. https://doi.org/10.1016/S0191-8869(00)00064-7.

Williams, L.M., Kemp, A.H., Felmingham, K., Liddell, B.J., Palmer, D.M., Bryant, R.A., 2007. Neural biases to covert and overt signals of fear: dissociation by trait anxiety and depression. J. Cogn. Neurosci. 19 (10), 1595–1608. https://doi.org/10.1162/jocn.2007.19.10.1595.

Wirsich, J., Benar, C., Ranjeva, J.P., Descoins, M., Soulier, E., Troter, A., Confort-Gouny, S., Liegeois-Chauvel, C., Guye, M., 2014. Single-trial EEG-informed fMRI reveals spatial dependency of BOLD signal on early and late IC-ERP amplitudes during face recognition. NeuroImage 100, 325–336. https://doi.org/10.1016/j.neuroimage.2014.05.075.

Yamasaki, H., LaBar, K.S., McCarthy, G., 2002. Dissociable prefrontal brain systems for attention and emotion. Proc. Natl. Acad. Sci. U. S. A. 99 (17), 11447–11451. https://doi.org/10.1073/pnas.182176499.

Yeo, B.T., Krienen, F., Sepulcre, J., Sabuncu, M., Lashkari, D., Hollinshead, M., Roffman, J., Smoller, J., Zöllei, L., Polimeni, J., Fischl, B., Liu, H., Buckner, R., 2011. The organization of the human cerebral cortex estimated by intrinsic functional connectivity. J. Neurophysiol. 106 (3), 1125–1165. https://doi.org/10.1152/jn.00338.2011.